

Autorotation Transfer of Training: Effects of Helicopter Dynamics

Scaramuzzino, P.F.; Pool, D.M.; Pavel, M.D.; Stroosma, O.; Quaranta, Giuseppe; Mulder, Max

DOI

[10.4050/JAHS.69.022007](https://doi.org/10.4050/JAHS.69.022007)

Publication date

2023

Document Version

Final published version

Published in

American Helicopter Society. Journal

Citation (APA)

Scaramuzzino, P. F., Pool, D. M., Pavel, M. D., Stroosma, O., Quaranta, G., & Mulder, M. (2023). Autorotation Transfer of Training: Effects of Helicopter Dynamics. *American Helicopter Society. Journal*, 69(2), Article JAHS-2289-Feb-2023. <https://doi.org/10.4050/JAHS.69.022007>

Important note

To cite this publication, please use the final published version (if applicable). Please check the document version above.

Copyright

Other than for strictly personal use, it is not permitted to download, forward or distribute the text or part of it, without the consent of the author(s) and/or copyright holder(s), unless the work is under an open content license such as Creative Commons.

Takedown policy

Please contact us and provide details if you believe this document breaches copyrights. We will remove access to the work immediately and investigate your claim.

Green Open Access added to TU Delft Institutional Repository

'You share, we take care!' - Taverne project

<https://www.openaccess.nl/en/you-share-we-take-care>

Otherwise as indicated in the copyright section: the publisher is the copyright holder of this work and the author uses the Dutch legislation to make this work public.

Autorotation Transfer of Training: Effects of Helicopter Dynamics

Paolo Francesco Scaramuzzino*
Flight Mechanics Engineer
Leonardo Helicopter Division
Cascina Costa di Samarate, Italy

Daan M. Pool
Assistant Professor
Delft University of Technology
Delft, The Netherlands

Marilena D. Pavel
Associate Professor

Olaf Stroosma
Senior Researcher
Delft University of Technology
Delft, The Netherlands

Giuseppe Quaranta
Full Professor
Politecnico di Milano
Milan, Italy

Max Mulder
Full Professor
Delft University of Technology
Delft, The Netherlands

This paper analyzes the effects of the helicopter dynamics on pilots' learning process and transfer of learned skills during autorotation training. A quasi-transfer-of-training experiment was performed with 10 experienced helicopter pilots in the SIMONA moving-base flight simulator at Delft University of Technology. Pilots had to control an in-house flight dynamics model setup to simulate two types of helicopter dynamics: (1) a "hard" dynamics characterized by a low autorotative flare index requiring high pilot control compensation and (2) a "easy" dynamics characterized by a high autorotative flare index with low pilot control compensation required. Two groups of pilots tested these types of dynamics in a different training sequence: hard-easy-hard (HEH group) and easy-hard-easy (EHE group). The main conclusion of this study proved that simulator training for autorotation can best start with pilots training in the most resource demanding condition. A more challenging helicopter's dynamics will require higher pilot agility and more rapid responses to his/her perceptual changes. This will result in pilots developing more robust and adaptable flying skills. Indeed, a clear positive transfer of training effect was observed in the experiment presented in this paper in terms of acquired pilot skills in the HEH group, but not the EHE group. Positive transfer was especially observed in terms of reduced rate of descent at touchdown. The two groups differed in the control strategy applied, with the HEH group having developed a control technique mimicking more closely the one adopted in a real helicopter.

Nomenclature

Roman symbols

df	number of degrees of freedom used in a statistical test
F	F -statistic in the analysis of variance
h	altitude, ft
K	scaling gain of the washout filter
N_{des}	number of landings within desired performance, - or % of the total number
N_{ad}	number of landings at least within adequate performance, - or % of the total number
p	p -value (significance)
p	roll rate, deg/s
q	pitch rate, deg/s
r	yaw rate, deg/s
t	t -statistic in the t -test
t	time, s
v	lateral speed, ft/s
V_{hor}	horizontal speed, kn
V_z	rate of descent, ft/min
U	U -statistic in the Mann-Whitney U test
Z	Z -statistic in the Wilcoxon signed-rank test

Greek symbols

δ_0	collective lever input, %
δ_{1s}	longitudinal cyclic stick input, %

ζ	damping ratio of the washout filter,
θ	pitch angle, deg
τ	time to contact, s
ϕ	roll angle, deg
Ω	main rotor speed, deg/s or % of the value at idle
ω_b	third-order break-frequency of the washout filter, rad/s
ω_n	natural break-frequency of the washout filter, rad/s

Subscripts

cush	cushion
f	failure
fl	flare
reac	reaction
rec	recovery
rot	rotation
td	touchdown

Introduction

Autorotation is a flight condition where the rotation of the rotor is sustained by the airflow moving up through the rotor, rather than by means of engine torque applied to the shaft. Helicopter pilots use autorotation following partial or total engine power failure to reach the nearest suitable landing site. The energy stored in the rotor is preserved at the expense of the helicopter's potential energy, that is, the altitude. Therefore, a helicopter can sustain autorotation only by means of descending flight.

Whether due to an actual emergency or during the training for such an event, autorotations often result in an accident in which the pilot fails

*Corresponding author: scaramuzzinopaolo@gmail.com.
 Manuscript received February 2023; accepted October 2023.

to perform the maneuver correctly, as reported by the accident analyses carried out by the U.S. Joint Helicopter Safety Analysis Team (Refs. 1,2) and the European Helicopter Safety Analysis Team (Refs. 3,4), in which the category “Forced (emergency) and practice (training) autorotations” appears as one of the main occurrences. These accidents were primarily due to the pilots’ lack of experience in make/model or the instructor pilot’s failure to intervene in time to prevent the accident.

Autorotation is thus considered to be a key critical training scenario (Refs. 5–7) and efforts to enhance helicopter safety need to be devoted towards the improvement of autorotation training in both primary and advanced flight training and the development of simulator programs to improve autorotation skills.

Full-down autorotations are seldom practiced during civil in-flight training, due to the high risks involved in the touchdown part of the maneuver. In the best case scenario, poorly executed autorotations during in-flight training may damage the helicopter. For this and other reasons, such as avoiding wearing out the skids, many flight schools prefer to teach only autorotations with a power recovery. A power recovery autorotation terminates in a hover as opposed to landing without power. This is always possible in a training situation because the engine failure is not real, but simulated by disengaging the rotor shaft from the power shaft by means of a clutch with the engine in an idle state.

Conversely from what one may think, there are also many risks involved in power recovery autorotations, especially when dealing with turbine engine helicopters. For most piston engine helicopters, switching from unpowered to powered flight is merely a matter of opening the throttle at the right time, while ensuring that the engine and the rotor do not overspeed. The situation for turbine engine helicopters is different, due to the presence of the governor, whose function is to keep a constant rotor speed (rotor rpm) during flight. The governor measures and regulates the speed of the engine (engine rpm) using a feedback controller on the error in rpm (the difference between the measured rpm and the reference value, which is 100%). The feedback on the error in rpm is slow (frequency of the order of 1 Hz) and hence cannot anticipate power demands in a timely manner. This means that the outcome of the maneuver may be very sensitive to the choice of the power recovery time. For example, immediately after the flare, the collective will be raised to cushion the landing. In this phase, the rotor is decelerating because the rotor energy is used to arrest any remaining descent rate after completion of the flare. Together with the rotor, the engine decelerates, so if the power is recovered at this stage, the governor will attempt to restore the rpm to 100% increasing the workload on the pilot, who has to coordinate the pedals to counteract the re-engagement of the engine and monitor the engine gauges at the time the pilot should be looking outside. So, a power recovery may cause more handling problems than landings without an engine, especially if the throttle is not opened at the right time, which is ideally at the start of the flare.

To overcome this issue, a synergistic approach between feedback on the error in rpm and feedforward on the collective input variation with respect to the trim value is usually adopted. A far more robust and reliable approach is proposed by Zheng et al. (Ref. 8), who used an engine nonlinear model predictive control, with an objective function that does not consider only the error in rpm but also the deviation between the torque provided by the power turbine and that demanded by the helicopter.

Whether a power recovery autorotation acts as valid replacement of an autorotation to touchdown depends on the part of the maneuver that the instructor intends to teach (Ref. 7). The fundamentals of airspeed control to transition from the entry to autorotation up to the flare are essential to be able to reach a specific spot on the ground (Ref. 9) and can be taught with a power recovery at the start of the flare. To avoid unrealistic practice from the flare to the touchdown, the maneuver should not terminate with a power recovery (Ref. 6).

This is true especially for helicopters with free turbine engines, that is, engines in which the power turbine is not mechanically linked to the compressor turbine. For this type of engine, the power turbine extracts power from the exhaust stream of the compressor turbine. This means that even in a ground idle setting, the engine is still burning fuel to keep the compressor turning and its hot exhaust gases are impinging on the power turbine, resulting in a residual turbine output power. If the turbine and rotor tachometer needles are split, the free-wheeling unit causes no power being transmitted to the rotor system. However, in the event of low rotor speed, the two needles are joined and some power will still be transmitted, resulting in an unrealistic practice because the helicopter appears lighter than it really is and the rotor system appears to have less drag than it really has and more inertia during the final flare. Indeed, the residual turbine output power delivered to the rotor contributes to the generation of lift to an extent proportionate to the size of the engine (e.g., for helicopters with relatively low disk loadings, such as the MD 500D, the helicopter appears 200/300 pound lighter than it really is (Ref. 6)). This will result in a higher *autorotative flare index* (Ref. 10) and hence a possibly easier autorotation. Therefore, when the pilot is exposed to a real power-out situation for the first time, the apparent loss in rotor performance can cause dramatic consequences.

This demonstrates the importance for the pilots to train with helicopters with different handling characteristics (e.g., different rates of descent, size, weight, rotor inertia, agile/sluggish dynamics) to be prepared for the unexpected because of the variety of conditions that pilots may face during emergencies requires experience and judgment in order to react promptly and avoid the many possible errors.

The high risks deriving from in-flight training for emergency situations, such as engine failures, are pushing the helicopter industry towards an ever-growing use of real-time flight simulation. Simulator training represents the only viable alternative to enable pilots to extensively practice hazardous scenarios in a safe environment. However, to avoid unrealistic training and negative transfer of skills when similar situations are encountered during actual flight, there is a need to bridge the gap between simulator scenarios and reality for edge-of-the-envelope flight.

One key challenge for obtaining representative simulation and effective pilot training in ground-based simulators is ensuring a sufficiently realistic flight model (Ref. 11). While this is true for flight simulation in general, the need for high-accuracy models is particularly acute for flight conditions that are the result of abnormal modes of operation, such as autorotation.

For example, the representation of the rotor wake plays an essential role in rotorcraft flight mechanics models. Houston and Brown (Ref. 12) have investigated how vorticity transport models, as opposed to the simpler finite-state induced velocity models (Ref. 13), affect modeling quality for autorotation. Ji et al. (Ref. 14) focused on the development of a novel low-altitude turbulence model, whereas Taymourtash et al. (Ref. 15) performed a wind-tunnel experiment to study the helicopter-ship aerodynamic interaction and used the experimental results to develop an identification algorithm to reconstruct the effect of the variation of the flow field due to the interaction between the airwake of the ship and the rotor-induced wake. Both these models can be integrated into high-fidelity simulation environments to improve pilot training of operations in low altitude and shipboard operations, respectively.

Furthermore, many studies have focused on the effects of the variable rotor angular speed in autorotation (Refs. 16–24) and in one-engine-inoperative conditions (Ref. 23), which are usually neglected in normal powered-flight rotorcraft models. Han et al. (Ref. 25) analyzed the effects of different types of gurney flaps on the performance of variable speed rotors, demonstrating their ability to yield power savings and expand the flight envelope, especially near-stall and high-speed flight.

Finally, key efforts were also devoted to model development and validation against wind tunnel and/or flight-test data in autorotation and the vortex ring state region for nonconventional helicopters, such as rotary decelerators of falling objects (e.g., ejection seat equipped with a folded rotor) (Refs. 26–28) and coaxial helicopters (Refs. 29, 30).

Besides model fidelity, pilots' perception and their use of available cues is another aspect that should not be underestimated in flight simulation for training purposes (Refs. 31–36). One of the most debated issues regarding simulator cueing is whether full-motion simulators are actually needed to achieve superior training quality. While this can be considered a general simulation question, there are peculiarities for each aircraft class, for example, fixed-wing, helicopters, that require to perform a specific assessment for each one of them. References 37 and 38 investigated the effects of a range of visual and motion cue settings on pilots' ability to perform unpowered helicopter landings. Both works showed that helicopter touchdown performance, along with pilot opinion, improved with increased motion fidelity. However, in-simulator performance and simulator acceptance by the pilots are not metrics of training effectiveness when no transfer paradigm is adopted. To overcome the inconsistency among the results of the individual studies on the need for motion bases (Ref. 39), de Winter et al. (Ref. 40) conducted a meta-analysis on 24 transfer-of-training experiments with motion as an independent variable, using both fixed- and rotary-wing aircraft models, showing that there is no overall evidence that motion improves performance in real aircraft, even though positive effects in favor of motion are observed in quasi-transfer studies and for individuals without flight experience learning disturbance-rejection tasks or maneuvers of vehicles with low dynamic stability, such as helicopters. Since then, other transfer-of-training experiments were performed for both fixed-wing aircraft (Refs. 32, 41) and helicopters (Refs. 42–46). Most of these experiments use a quasi-transfer paradigm, where trained skills are applied on a simulator with capabilities that are beyond those of a typical training simulator (Ref. 47), corroborating the assumption that such simulators act as a valid replacement for the actual aircraft. Similar results are obtained in all these studies: the need for simulators with a motion system cannot be claimed. On the contrary, subjects who trained in poorer cueing situations developed control strategies that were revealed to be adaptable to higher fidelity conditions.

Despite these recent efforts devoted to achieving more accurate rotorcraft models and clarifying the relation between simulator cueing and training effectiveness, only a few studies have explicitly investigated the effects of rotorcraft model fidelity and dynamics variations on pilot behavior and (transfer of) training, for example, Refs. 46 and 48–50. Especially for a critical hands-on maneuver such as autorotation, pilots need to adjust their control strategy according to the helicopter dynamics they control (Refs. 47, 51, 52). Helicopters with different handling characteristics may require very different skills from pilots to accomplish the task. Earlier experiments in training a lateral sidestep hover maneuver (Ref. 48) showed that flight-naïve participants—that is, without any previous real or simulated flight experience—are more likely to develop robust and flexible flying skills when they start the training in a helicopter with agile system dynamics. According to Nusseck et al. (Ref. 48), starting the training of a certain task with the most challenging configuration provides the pilot with the ability to accomplish the same task with every other configuration after a short adaptation phase. A similar result was observed by Scaramuzzino et al. (Ref. 46) with experienced pilots during the training of the straight-in autorotation maneuver with a four degrees-of-freedom (DOF) helicopter model, consisting of 3-DOF longitudinal dynamics plus rotor speed DOF.

This paper investigates whether the acquisition of flying skills for autorotation, and their transfer, is affected by the helicopter dynamics. Two helicopter configurations, characterized by a different autorotative flare index and a different level of intervention required by the pilot were

considered: “hard,” with low index and high pilot control compensation required, and “easy,” with high index and low control compensation required. It was hypothesized that dynamics that require more control compensation may lead to the development of a more robust control behavior, one that can be easily adapted to a helicopter with different dynamics, yielding substantial benefits in terms of engine failure handling capabilities. The results of a quasi-transfer-of-training experiment with 10 experienced helicopter pilots, divided into two groups, performed in TU Delft's SIMONA Research Simulator (SRS) are presented to corroborate this hypothesis. The helicopter's final states, that is, attitudes and linear and rotational rates, have been used to compare the performance at touchdown. Additionally, a recently developed method, referred to as control event detection (CED) (Ref. 46), is used to perform an in-depth analysis of pilot control actions involved in a successful autorotative landing.

Methods

Task

In rotorcraft handling quality research, experimental tasks are usually defined according to the specifications of the mission-oriented design standard, ADS-33E (Ref. 53). Although conceived for military rotorcraft, ADS-33E is widely used to assess handling qualities characteristics of commercial rotorcraft as well (Refs. 54–57), as there is no counterpart in the civil domain. However, the use of ADS-33E mission task elements (MTEs) is not always relevant, especially in the design of training tasks. Furthermore, ADS-33E does not have a specific autorotation maneuver MTE. Since there are no specific handling quality metrics for autorotation, pilot-in-the-loop autorotation maneuvers are usually evaluated based on subjective pilot feedback and comments and on objective measurements of landing survivability metrics (Ref. 58).

For this experiment, an MTE was defined for the straight-in autorotation maneuver; the proposed test course is shown in Fig. 1. The simulation starts with the helicopter trimmed in straight level flight at 60 kn air speed, at an altitude of 1,000 ft. The symmetry plane of the helicopter is aligned with the center line of a runway, whose starting point is located 3,281 ft (1,000 m) ahead of the helicopter initial position. The pilot has to keep a constant speed and altitude until the power failure is triggered from the control room. As soon as the pilot recognizes the unannounced failure, he has to recover starting a steady descent in autorotation, maintaining 60 kn airspeed and keeping the rotor RPM in the green arc of the tachometer. When close enough to the ground, the pilot has to flare in order to reduce both the rate of descent and the forward speed. They finally level the skids with the ground, to avoid a tail strike, and pull-up the collective to cushion the touchdown. In the simulator, the contact forces at touchdown were not modeled. Therefore, the simulation stopped automatically once the center of gravity of the helicopter reached 2 m above the ground.

Performance standards for the straight-in autorotation maneuver are adapted from Sunberg et al. (Refs. 58, 59) and are listed in Table 1. The values of the horizontal speed and the rate of descent at touchdown refer to the AH-1G helicopter (Ref. 58), which has a similar skid landing gear as the baseline helicopter (Bo-105) considered in this paper. Therefore, these were not changed. Although characterized by a similar landing system, the AH-1G and the Bo-105 are different helicopters, with different performance and intended role. Indeed, the AH-1G is a two-bladed rotor, single-engine attack helicopter, whereas the Bo-105 is a light, twin-engine, multipurpose helicopter with a four-bladed hingeless rotor. The maximum values of the pitch angle at touchdown, which are responsible for preventing tail strike, were slightly increased due to the different helicopter geometry. Desired performance translates into a successful landing, that is, the helicopter's final state at ground contact is

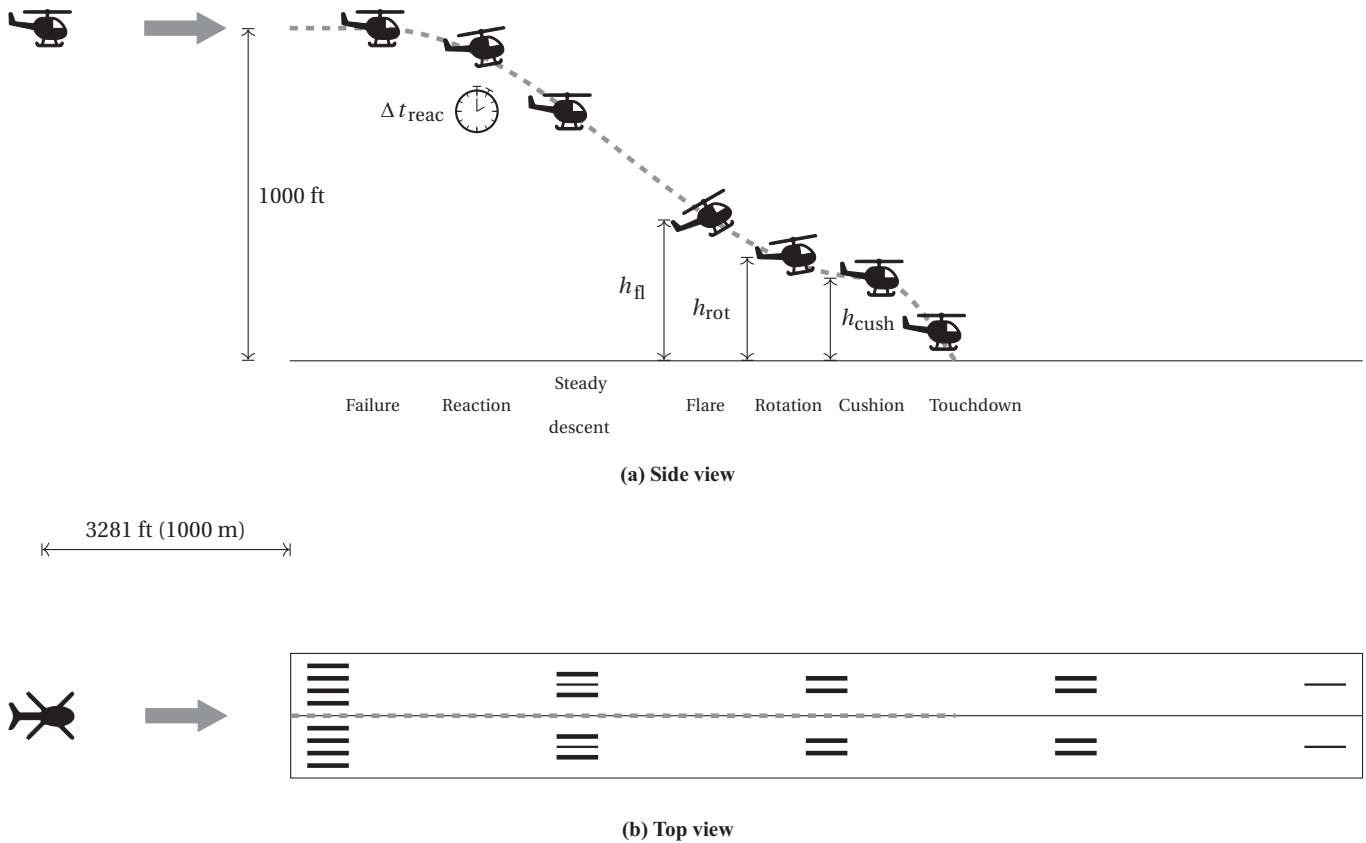


Fig. 1. Suggested course for straight-in autorotation maneuver.

Table 1. Performance: Straight-in autorotation maneuver (adapted from Ref. 58)

Metric	Performance			
	Desired		Adequate	
	Minimum	Maximum	Minimum	Maximum
Roll angle at touchdown ϕ_{td} (deg)	-5	5	-10	10
Pitch angle at touchdown θ_{td} (deg)	-5	12	-5	18
Forward speed at touchdown $V_{x_{td}}$ (kn)	0	30	0	40
Lateral speed at touchdown v_{td} (ft/s)	-6	6	-12	12
Rate of descent at touchdown $V_{z_{td}}$ (ft/min)	0	480	0	900
Roll rate at touchdown p_{td} (deg/s)	-8	8	-15	15
Pitch rate at touchdown q_{td} (deg/s)	-10	10	-20	20
Yaw rate at touchdown r_{td} (deg/s)	-8	8	-15	15

such that the survivability of aircraft and crew are not threatened. Adequate performance translates into marginal landing conditions that would likely result in damage to the aircraft, but be survivable to the occupants and the equipment. The values presented in Table 1 are defined according to landing survivability metrics that are based on specifications for military helicopters’ structural design (Refs. 60,61) and the accident analysis conducted by Crist and Symes (Ref. 62).

Helicopter dynamics

Participants performed the straight-in autorotation task by controlling a 7-DOF (6-DOF rigid-body dynamics plus rotor speed DOF), nonlinear, and generic helicopter model with quasi-steady flapping dynamics and uniform inflow (Ref. 63) through a cyclic stick, a collective lever, and rudder pedals. Especially the assumption of uniform distribution of the

induced velocity on the rotor disk is strong for autorotative flight in forward translation, but was deemed acceptable as Murakami and Houston (Ref. 64) showed that finite-state, dynamic inflow modeling for autorotation does not affect neither the helicopter trim states nor its dynamics unless in steep descents with low forward speed. This generic model can be used in combination with different parameter sets to approximate the dynamic response of any conventional helicopter configuration.

From the wide range of configurations studied by Scaramuzzino et al. (Ref. 24), two were selected for a previous study (Ref. 46), in which a 4-DOF (3-DOF longitudinal dynamics plus rotor speed DOF) helicopter model was used. The “hard” dynamics are representative of the Bo-105 helicopter, and the flight model parameters were taken from Padfield (Ref. 65). The “easy” dynamics represent a variation of the Bo-105 helicopter with reduced weight in order to achieve a higher autorotative flare index (Ref. 10). The same configurations were considered in the current

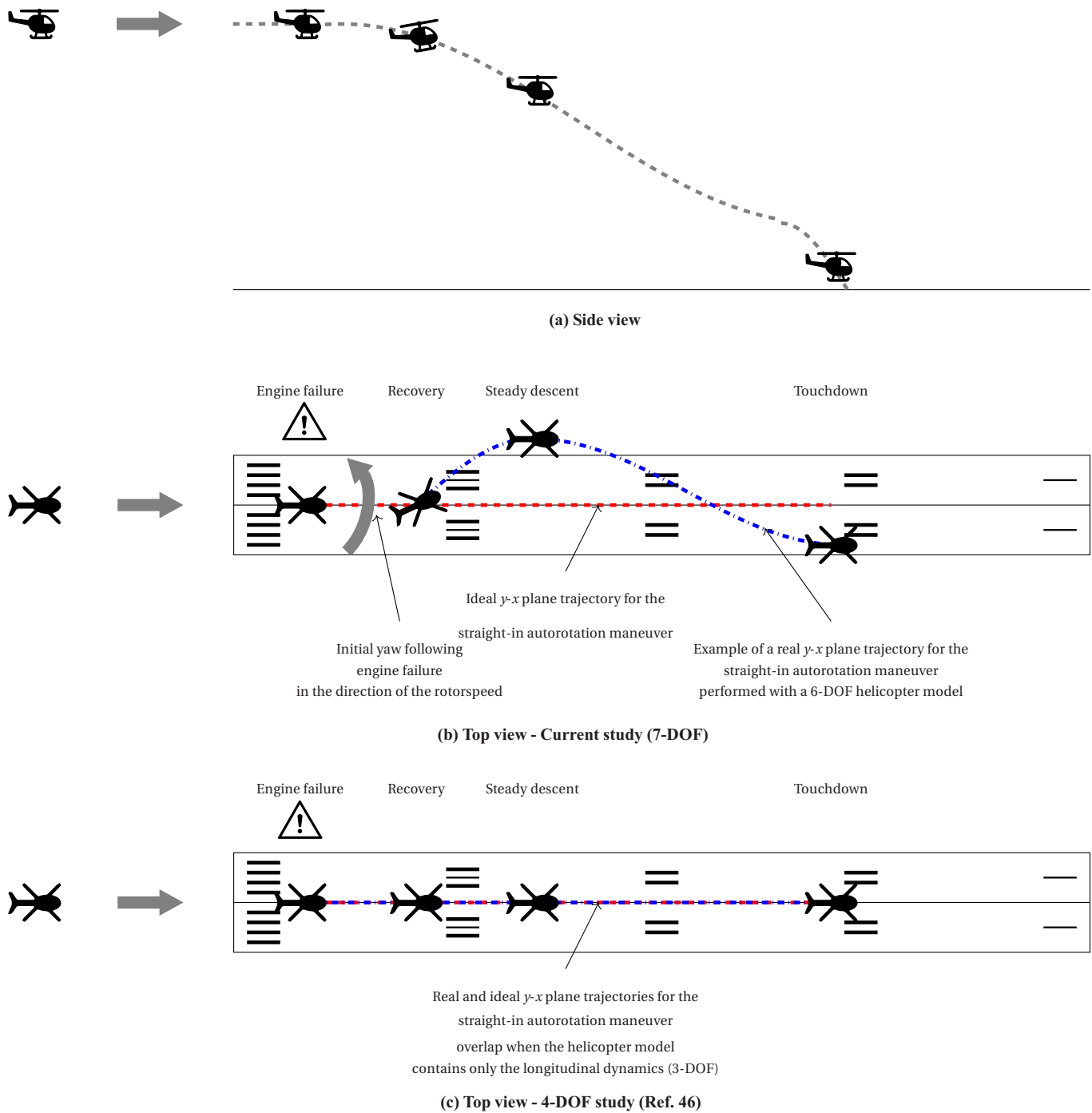


Fig. 2. Comparison in terms of helicopter model between the current study and the previous one (Ref. 46).

Table 2. Experiment phases

Phase	HEH Group	EHE Group	Duration (Number of Autorotative Landings)	Motion
Familiarization	Hard helicopter dynamics	Easy helicopter dynamics	3	Off
Training	Hard helicopter dynamics	Easy helicopter dynamics	15	On
Transfer	Easy helicopter dynamics	Hard helicopter dynamics	15	On
Back-transfer	Hard helicopter dynamics	Easy helicopter dynamics	15	On

Table 3. Participants

Participant ID	HEH Group		EHE Group	
	Age	Flight Hours	Age	Flight Hours
1	19	100	58	190
2	46	5,600	34	400
3	53	140	44	3,000
4	55	320	56	1,200
5	45	2,000	45	400
Avg	43.6	1,632	47.4	1,038
Std	14.4	2,355	9.8	1,163

experiment to corroborate the results of Scaramuzzino et al. (Ref. 46), which were obtained with a 3-DOF helicopter model. The differences in terms of visual and motion stimuli between the current and the previous study (Ref. 46) due to the different helicopter models are illustrated in Fig. 2. More details about audio, visual, and motion stimuli provided to the pilots during the experiment are given in sections Apparatus and Motion Filter Tuning.

While similar in terms of stability characteristics, these two configurations proved to be considerably different in terms of handling qualities during a preexperiment with a test pilot, both concerning objective

metrics of performance at touchdown (Table 1) and subjective handling quality ratings provided by the pilot (Ref. 46).

Experiment structure

The experiment is structured as indicated in Table 2 and consists of four phases:

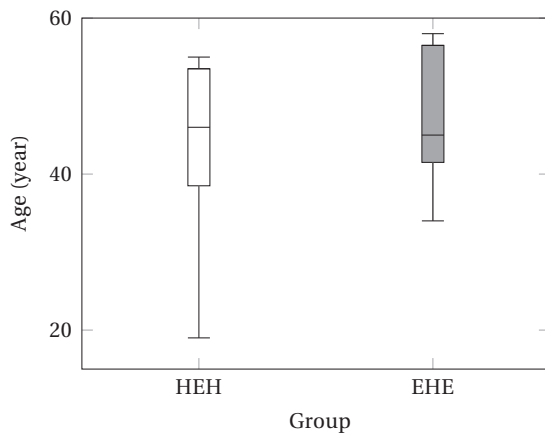
1) *Familiarization*: This phase was intended to help the participants get acquainted with the simulation environment (helicopter model, cockpit ergonomics, control inceptors, etc.). For this reason, the simulator motion system was disabled to reduce the chances of exceeding the simulator’s physical limits due to a potential loss of control in the first runs of the experiment and each participant performed the task with either the hard or the easy helicopter dynamics. These runs were not used in the analysis.

2) *Training*: Each participant performed the task with the same helicopter dynamics used during the familiarization phase. Starting from this session, the simulator motion system was enabled.

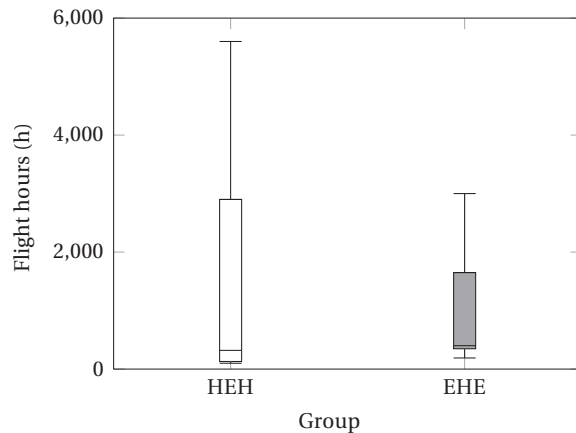
3) *Transfer*: Each participant performed the task with the other helicopter configuration.

4) *Back-transfer*: Each participant performed the task with the initial hard/easy helicopter configuration.

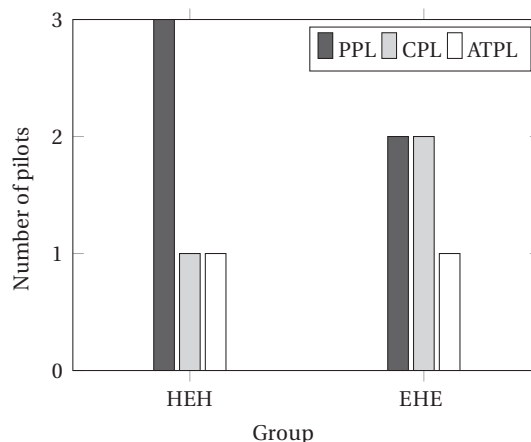
In total, the complete experiment session for each participant lasted approximately 3 h.



(a) Age distribution among the two groups



(b) Flight hours distribution among the two groups



(c) License-type distribution among the two groups

Fig. 3. Comparison in terms of age, flight hours, and license type between the two groups.

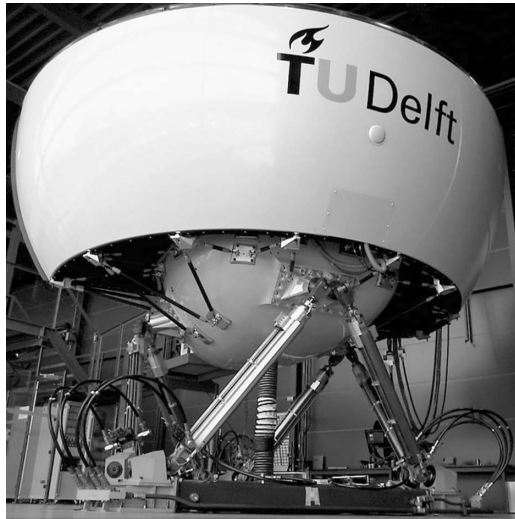


Fig. 4. The SIMONA research simulator at Delft University of Technology.

Table 4. The SIMONA Research Simulator workspace per degree of freedom

DOF	Minimum	Maximum
Surge (m)	-0.981	1.259
Sway (m)	-1.031	1.031
Heave (m)	-0.636	0.678
Roll (deg)	-25.9	25.9
Pitch (deg)	-23.7	24.3
Yaw (deg)	-41.6	41.6

Dependent measures

To investigate the effect of the helicopter dynamics (independent variable) on autorotation performance and training, the dependent measures related to the MTE definition presented in Table 1 were considered. Since those measures assess only the performance at touchdown, other metrics were also taken into account to compare the control strategies adopted by the participants of the two experiment groups, namely,

- 1) Number of landings at least within adequate performance (Table 1),
- 2) Number of landings within desired performance (Table 1),
- 3) *Reaction time*: time required by the pilot to lower the collective after engine failure (Fig. 1),
- 4) *Flare initiation altitude*: altitude at which the pilot initiates the flare by pulling back the cyclic stick (Fig. 1),
- 5) *Rotation altitude*: altitude at which the pilot levels the skids with the ground by pushing forward the cyclic stick (Fig. 1), and
- 6) *Cushion altitude*: altitude at which the pilot raises the collective to cushion the touchdown (Fig. 1).

Metrics 3–6 were extracted from the experiment time histories using a previously developed CED methodology (Ref. 46).

Hypotheses

For this experiment, only one main hypothesis was tested. Based on previous experimental evidence (Refs. 46, 48) and current in-flight training procedures, it is envisioned that pilots who start the training with the most challenging configuration (hard dynamics) are more likely to

develop robust and flexible autorotation skills that can be easily adapted to different helicopter configurations and dynamics. Therefore, it is expected that flying skills are positively transferred from the hard to the easy dynamics, but not the reverse. When positive transfer happens, we expect to see lower rates of descent after transition to a different dynamics, as a lower descent rate is a key indicator for a controlled and smooth touchdown (Ref. 7). Among all the dependent measures, the rate of descent is thus expected to cover a key role to corroborate our hypothesis.

The similarities with a previous study (Ref. 46) conducted with a 4-DOF (3-DOF longitudinal dynamics plus rotor speed DOF) helicopter model can be used to formulate a set of secondary hypotheses. Since the final part of the autorotation is mainly a longitudinal maneuver, we expect similar trends in terms of pilots' control strategy, whereas we envision lower reaction times after failure in the current experiment because the most important cue that is used by pilots to recognize an engine failure, that is, the initial yaw in the direction of the rotor angular speed, could not be modeled in the previous experiment (Ref. 46).

Participants

A total of 10 experienced helicopter pilots with different backgrounds (license type) and a mix of civil and military experience took part in the experiment; all of them were male. The participants had an average age of 45.5 years ($\sigma = \pm 11.8$ years) and an average helicopter experience of 1,335 flight hours ($\sigma = \pm 1,778$ flight hours), ranging from a minimum of 100 to a maximum of 5,600 flight hours. Participants were divided into two groups in such a way that they had, on average, a comparable number of flight hours and a similar distribution, as shown in Table 3 and Fig. 3. Besides the number of flight hours, pilots background was also considered during the separation of the pilots in the two groups (Fig. 3(a)).

Participants signed an informed consent prior to the experiment. The experiment has been approved by the Human Research Ethics Committee of Delft University of Technology under approval letter number 1423.

Apparatus

The experiment was conducted in the SRS (Fig. 4), which is a moving-base simulator at the Faculty of Aerospace Engineering of TU Delft (Ref. 66). The SRS is equipped with a 6-DOF hydraulic motion system, which was used in the experiment to provide motion cues. The operational stroke of the motion system actuators is ± 0.575 m, whereas their speed limit is ± 1 m/s. The resulting workspace limits on the 6 DOF are summarized in Table 4.

In terms of visual equipment, the SRS is fitted with a $180^\circ \times 40^\circ$ 3-projector Digital Light Processing (DLP[®]) collimated display. A representative out-of-the-window scene was presented on this display (Fig. 5(a)). Furthermore, an instrument panel (Fig. 5(b)), consisting of a tachometer, airspeed indicator, artificial horizon, altimeter, turn and slip indicator, compass and vertical speed indicator, and a control loading trim display (Fig. 6) were projected on two monitors inside the cockpit. Pilots use the trim display only before the start of each run in order to find the trim position of all the flight controls. This enables them to keep the initial equilibrium condition (straight level flight at 60 kn) and avoid a transient response at the start of the simulation.

The right seat of the cockpit is equipped with realistic helicopter control inceptors with a programmable control loading system, whose parameters are set as reported in Table 5 after consultation with test pilots (Ref. 67).

The rotor sound is played during the simulation to increase immersion. The sound is modulated based on the value of the rotor RPM, so that



Fig. 5. Out-of-the-window scenery and instrument panel used for the current experiment.

Table 5. Control loading settings

Parameter	Longitudinal Cyclic	Lateral Cyclic	Collective
Periodic			
Forward friction level (N)	2.0	2.0	6.0
Positive forward stop (deg)	15.0	15.0	16.0
Negative forward stop (deg)	-15.0	-15.0	-16.0
Nonperiodic			
Linkage stiffness (N/deg)	50.0	50.0	50.0
Linkage damping (N s/deg)	0.01	0.01	0.01
Positive aft travel limit (deg)	14.8	14.8	15.8
Negative aft travel limit (deg)	-14.8	-14.8	-15.8
Aft friction (N)	2.0	2.0	6.0
Aft inverse damping (deg/N/s)	10.0	10.0	10.0
Second feel spring slope (N/deg)	3.0	3.0	0.0
Breakout level (N)	0.0	0.0	0.0

Table 6. Motion cueing settings

DOF	High-Pass Filter					Low-Pass Filter (Tilt Coordination)		
	K	ω_n (rad/s)	ζ	ω_b (rad/s)	Order	ω_n (rad/s)	ζ	Order
Longitudinal dynamics								
Heave	0.5	3.5	0.7071	0.2	3	-	-	-
Surge	0.5	1.5	0.7071	0.0	2	3.0	0.7071	2
Pitch	0.5	1.5	0.7071	0.0	2	-	-	-
Lateral-directional dynamics								
Yaw	0.5	1.5	0.7071	0.0	2	-	-	-
Sway	0.5	1.5	0.7071	0.0	2	3.0	0.7071	2
Roll	0.5	1.5	0.7071	0.0	2	-	-	-

the participant can use sound cues as a source of information to control the rotor RPM, rather than by looking at the instrument panel. Moreover, a low-RPM acoustic warning is activated every time the rotor speed drops below 85%. The low-RPM warning is used as a backup cue for the rotor sound so that the failure can be recognized without necessarily looking at the instruments. Engine sound is not included.

Motion filter tuning

The classical washout algorithm is used to map the vehicle motion on the simulator workspace (Ref. 68). The three high-pass filters related

to the longitudinal dynamics (the pitch, surge, and heave axes) are set according to the tuning conducted by Scaramuzzino et al. (Ref. 46) on a 4-DOF (3-DOF longitudinal dynamics plus rotor speed DOF) helicopter model. So these filters are selected to be of second order for the pitch and surge axes and of third order for the heave axis. Although surge and heave axes are both translational DOF, a different order of the filter is selected for these two axes. Indeed, a second-order high-pass filter along the surge axis allows to achieve sufficient washout through the use of tilt coordination. This was first observed by Reid and Nahon (Ref. 69) and reiterated by Grant and Reid (Ref. 70). Therefore, the combination of the tilt coordination and the body to inertial transformation effectively adds one order of washout.

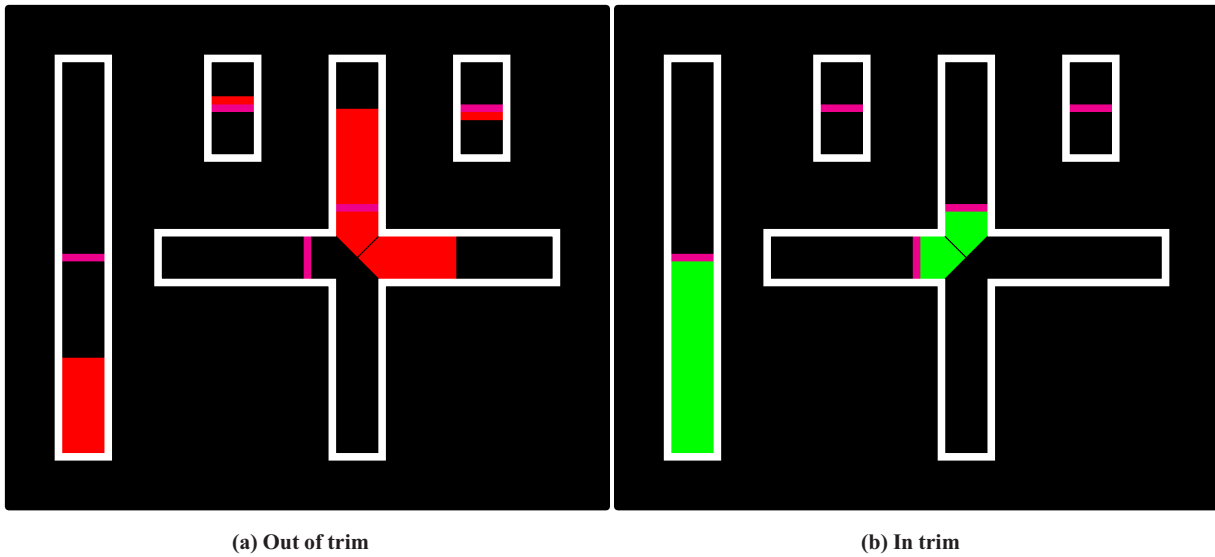


Fig. 6. Trim display.

The high-pass filter parameters related to a rotational DOF in the lateral-directional dynamics (the roll and yaw axes) are set equal to those along the pitch axis. The high-pass filter parameters related to the sway axis are set equal to those along the surge axis. The complete motion filter settings for the 6 DOF are presented in Table 6.

Data processing and analysis

Prior to performing the statistical tests, all the dependent measures defined in the section Dependent measures, except the number of landings at least within adequate performance and within desired performance, were averaged over the last 10 runs of each phase for every participant. Mixed repeated measures ANOVA (analysis of variance) tests were conducted on all the dependent variables, considering the experiment phases as the main within-subjects factor, characterized by three levels: training, transfer and back-transfer, and the groups as the main between-subjects factor, characterized by two levels: hard-easy-hard (HEH) and easy-hard-easy (EHE). Before conducting the statistical tests, the fulfillment of the ANOVA assumptions, that is, normality (i.e., data follow a normal distribution) and sphericity (i.e., data exhibit the similar values of variance), was verified. Regarding the normality assumption, some skewness in the data was accepted, as long as it was reasonably small. Indeed, the ANOVA is a robust technique and should also still provide reliable results in the presence of minor violations. For variables in which sphericity was violated according to Mauchly’s test, we adopted either the Greenhouse–Geisser correction, when the Greenhouse–Geisser estimate of sphericity ϵ is below 0.75 ($\epsilon < 0.75$), or the Huynh–Feldt correction, when the Greenhouse–Geisser estimate of sphericity ϵ is above 0.75 ($\epsilon > 0.75$).

In the event of a statistically significant interaction effect between the two main factors (within- and between-subjects factors), main effects may provide misleading information (Ref. 71). Therefore, the so-called *simple* main effects are investigated. Dependent-samples *t*-tests between the phases of the experiment for each group are used to investigate the simple within-subjects effect and independent-samples *t*-tests between the groups in each phase are adopted to examine the simple between-subjects effect. If the interaction effect between the two main factors is not statistically significant, the two main effects are analyzed and if either of them is statistically significant, the respective simple main effect

is investigated accordingly. This process is shown in the flowchart of Fig. 7.

Results

Results are presented in the following using box-whiskers plots. On each box, the horizontal line represents the median over different data points. The box is delimited by the first and third quartiles; therefore, it includes data points between the 25th and the 75th percentile. The difference between the first and third quartiles defines the interquartile range. The two edges of the whiskers indicate the lowest and the highest data point within 1.5 of the interquartile range. All the data points not included in the whiskers are considered as outliers and represented by cross markers.

Statistically significant results of the *t*-tests are shown as follows. A curly brace with an asterisk on top is used to indicate a statistically significant difference between the two groups in a specific phase of the experiment. A curved arrow with an asterisk on the left indicates a statistically significant transfer-of-training effect for a specific group.

Performance scores

Table 7 summarizes the results of the repeated measures ANOVA tests for the different dependent measures considered in this study. This test was not performed on the number of landings within desired performance because this metric does not meet the assumption of normal distribution of the data required by the ANOVA test.

Figure 8 shows the number of landings at least within adequate performance N_{ad} and those within desired performance N_{des} for each group in each phase. Figure 8(a) illustrates that participants of both groups were able to attain at least adequate performance, that is, a survivable landing, in most of the experiment runs. However, the HEH group shows higher within-group variability than the EHE group. This is particularly true for the training and the back-transfer phases, where the EHE group controls the easy dynamics.

The number of survivable landings for the participants of the HEH group increases during the transfer phase and slightly decreases during the transition from the transfer to the back-transfer phase. The opposite is observed for the participants of the EHE group: the number of survivable landings decreases during the transfer phase and increases again

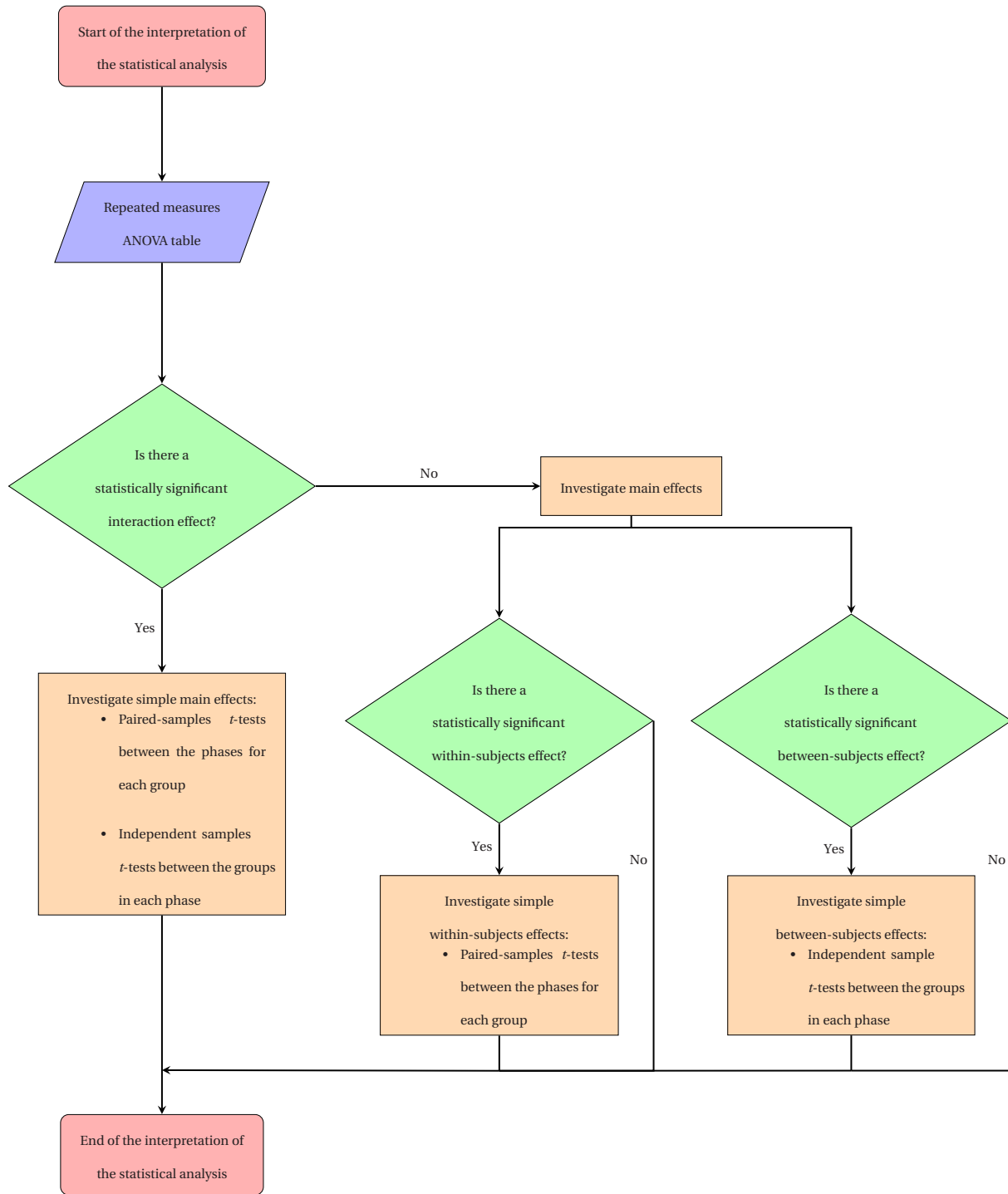


Fig. 7. Flowchart explaining the interpretation of the statistical analysis.

during the back-transfer phase to values comparable to those of the training phase. Figure 8(a) suggests that for the HEH group there is a positive transfer of training from the hard configuration to the easy configuration and no transfer of training from the easy configuration to the hard configuration. Although not statistically significant, a similar trend is also observed for the EHE group.

Participants of both groups struggled to attain desired performance (i.e., a successful landing) as shown in Fig. 8(b). This is most likely due to poor or lack of visual cues. Indeed, the SRS was conceived for

fixed-wing simulation and is not equipped with chin bubbles. As a consequence, pilots completely lose sight of the ground during the flare. Therefore, pilots either opt for a less effective flare, ending-up with a higher horizontal speed, or risk either to strike the tail on the ground or not to coordinate the cushion timely, resulting in a higher rate of descent at touchdown (Ref. 46). Nonetheless, the number of successful landings conveys the same information as the number of survivable landings, that is, a positive transfer of training is observed for both groups from the hard configuration to the easy configuration, but not the opposite.

Table 7. Repeated measures ANOVA results for all the dependent variables

Dependent Variable	Between Subjects Factor (Group)			Within Subjects Factor (Phase)			Within Subjects Interaction (Phase*Group)		
	df	F	Sig.	df	F	Sig.	df	F	Sig.
N_{ad}	1	0.570	0.472	2	2.439	0.119	2	4.195	0.034*
$\bar{\theta}_{td}$	1	2.156	0.180	2	0.548	0.589	2	0.862	0.441
$\bar{V}_{hor_{td}}$	1	7.750	0.024*	2	0.716	0.504	2	2.302	0.132
$\bar{V}_{z_{td}}$	1	1.072	0.331	2	1.490	0.255	2	5.487	0.015*
\bar{q}_{td}	1	4.345	0.071	2	0.459	0.640	2	0.804	0.465
$\bar{\phi}_{td}$	1	2.492	0.153	2	0.367	0.698	2	0.624	0.548
\bar{v}_{td}	1	0.144	0.714	2	0.597	0.562	2	1.593	0.234
\bar{p}_{td}	1	0.107	0.752	2	0.820	0.458	2	3.615	0.051
\bar{r}_{td}	1	2.459	0.155	2	0.398	0.678	2	0.644	0.538
$\Delta \bar{t}_{reac}$	1	0.032	0.863	1,290 ^{hf}	2.546	0.137	1,290 ^{hf}	0.262	0.679
\bar{h}_{fl}	1	2.136	0.182	2	0.479	0.628	2	2.087	0.157
\bar{h}_{rot}	1	0.170	0.691	2	7.179	0.006*	2	5.855	0.012*
\bar{h}_{cush}	1	1.999	0.195	2	0.077	0.926	2	3.947	0.040*
$\bar{\Omega}_{td}$	1	2.543	0.149	2	0.592	0.565	2	2.354	0.127

*Statistically significant ($p < 0.05$) difference between compared samples.

^{hf}Huynd-Feldt correction applied.

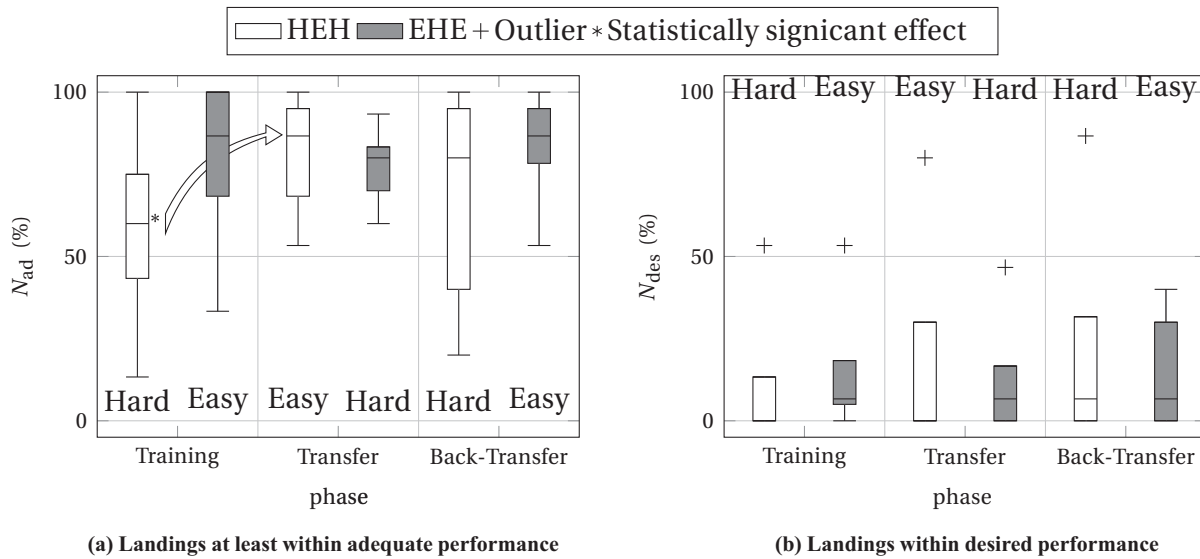


Fig. 8. Distribution of the number of landings at least within adequate performance and that within desired performance for each group in each phase.

Table 7 highlights a statistically significant interaction effect in terms of number of survivable landings N_{ad} (interaction effect: $F(2, 16) = 4.195$, $p = 0.034$), which was further investigated by performing t -tests on individual sets of samples. Tables 8 and 9 illustrate the results of these tests. A significant difference in terms of survivable landings only occurs between the training and the transfer phase for the HEH group (from the hard to the easy helicopter dynamics: $t(4) = -3.157$, $p = 0.034$). This partially confirms what has already been observed from Fig. 8(a).

The effectiveness of the training was further investigated by averaging the performance metrics defined in the section Task (longitudinal metrics: horizontal speed, rate of descent, pitch angle, and pitch rate at touchdown; lateral metrics: roll angle, lateral speed, roll rate, and yaw rate at touchdown) over the last 10 runs completed by each participant in each phase. The longitudinal and the lateral-directional metrics are shown in Figs. 9 and 10, respectively, as box-whiskers plots to compare

the performance of the two groups in the training, transfer, and back-transfer phases.

Figures 9(a) and 9(c) show the distribution of the average horizontal speed $\bar{V}_{x_{td}}$ and of the average pitch angle $\bar{\theta}_{td}$ at touchdown, respectively. The strong correlation between these two metrics is a key indicator of the flare effectiveness adopted by the two groups. The participants of the HEH group touched down with a higher pitch angle than those of the EHE group, meaning that they opt for a less effective flare, which translates into a lower horizontal speed at touchdown. Despite this clear difference between the two groups for both metrics, the repeated measures ANOVA tests of Table 7 highlight a statistically significant between-subjects effect only for the average horizontal speed at touchdown ($F(1, 8) = 7.750$, $p = 0.024$) that was further investigated by performing t -tests on individual sets of samples. Table 9 summarizes the results of these tests, highlighting the presence of a significant difference in the average horizontal

Table 8. Dependent-samples *t*-test between the experiment phases. Bonferroni correction was not applied

Metric	Group	From	To	<i>t</i> -test			From	To	<i>t</i> -test		
				t	df	Sig. (Two-tail.)			t	df	Sig. (Two-tail.)
N_{ad}	HEH	Train.	Transf.	-3.157	4	0.034*	Transfer.	Back-	1.907	4	0.129
	EHE			0.343	4	0.749		transfer	-1.826	4	0.142
$\bar{V}_{z_{td}}$	HEH	Train.	Transf.	3.998	4	0.016*	Transf.	Back-	-1.666	4	0.171
	EHE			-1.715	4	0.162		transfer	2.063	4	0.108
\bar{p}_{td}	HEH	Train.	Transf.			0.500 ^a	Transf.	Back-	0.445	4	0.679
	EHE			0.333	4	0.756		transfer	-2.797	4	0.049*
\bar{h}_{rot}	HEH	Train.	Transf.	1.299	4	0.264	Transf.	Back-	-0.715	4	0.514
	EHE			0.546	4	0.614		transfer	-3.414	4	0.027*
\bar{h}_{cush}	HEH	Train.	Transf.	1.659	4	0.172	Transf.	Back-	-1.894	4	0.131
	EHE			-9.614	4	0.001**		transfer	0.885	4	0.426

Abbreviations: tail., tailed; Train., Training; Transf., Transfer.

*Statistically significant ($p \leq 0.05$) difference between compared samples.

**Statistically highly significant ($p \leq 0.001$) difference between compared samples.

^aAt least one sample is not normally distributed. Related-samples Wilcoxon signed-rank test was applied instead of paired-samples *t*-test.

Table 9. Independent-samples *t*-test between the two groups

Metric	Phase	<i>t</i> -test		
		t	df	Sig. (Two-tail.)
N_{ad}	Training	-1.150	8	0.283
	Transfer	0.405	8	0.696
	Back-transfer	-0.934	8	0.378
$V_{hor_{td}}$	Training			0.056 ^a
	Transfer	-4.406	8	0.002*
	Back-transfer	-0.946	8	0.372
$V_{z_{td}}$	Training	1.672	8	0.133
	Transfer	0.331	8	0.749
	Back-transfer	1.056	8	0.322
q_{td}	Training	-4.420	8	0.002*
	Transfer			0.095 ^a
	Back-transfer	-0.554	8	0.595
p_{td}	Training			0.690 ^a
	Transfer	0.093	8	0.928
	Back-transfer	-1.380	8	0.205
\bar{h}_{rot}	Training	0.971	8	0.360
	Transfer	0.760	8	0.469
	Back-transfer	-0.367	8	0.723
\bar{h}_{cush}	Training	-0.549	5.147	0.606
	Transfer	-2.552	8	0.034*
	Back-transfer	-0.943	8	0.373

*Statistically significant ($p \leq 0.05$) difference between compared samples.

^aAt least one sample not normally distributed. Independent-samples Mann-Whitney U test was applied instead of independent-samples *t*-test.

speed at touchdown $\bar{V}_{x_{td}}$ between the two groups only during the transfer phase ($t(8) = -4.406, p = 0.002$). Although not significant, the difference between the two groups also seems consistent during the training phase, as can be confirmed by a Mann-Whitney U test ($U = 3, p = 0.056$).

A completely different trend can be observed for the average rate of descent at touchdown $\bar{V}_{z_{td}}$, as shown in Fig. 9(b). The HEH group exhibits an improvement from the hard (training phase) to the easy dynamics (transfer phase), whereas performance is unaffected going from the easy (transfer phase) to the hard dynamics (back-transfer phase).

Although less evident, a similar variation is found for the EHE group, whose performance degrades from the easy (training phase) to the hard dynamics (transfer phase) and improves from the hard (transfer phase) to the easy dynamics (back-transfer phase). These results suggest a correlation between the average rate of descent at touchdown and the number of survivable landings, as they are both characterized by a similar improvement trend from the hard to the easy configuration, but not the opposite. This improvement trend is confirmed by the repeated measures ANOVA test performed on the average rate of descent at touchdown, shown in Table 7 (statistically significant interaction effect: $F(2, 16) = 5.487, p = 0.015$) and was further investigated by performing *t*-tests on individual sets of samples. Tables 8 and 9 summarize the results of these tests, highlighting the presence of a significant difference in the average rate of descent $\bar{V}_{z_{td}}$ between the training and the transfer phase for the HEH group (from the hard to the easy helicopter dynamics: $t(4) = 3.998, p = 0.016$).

The surprising result concerns the average pitch rate at touchdown \bar{q}_{td} , which is strikingly different between the two groups during the training and the transfer phases, as shown in Fig. 9(d). Although not significant, the difference between the two groups is confirmed by a low between-subjects *p*-value in the repeated measures ANOVA test of Table 7 ($F(1, 8) = 4.345, p = 0.071$).

The presence of an overall significant effect in the complete data set of the average pitch rate was further investigated by performing *t*-tests on individual sets of samples. Table 9 illustrates the results of these tests and highlights a statistically significant difference between the two groups only during the training phase ($t(8) = -4.420, p = 0.002$). Although not significant, the difference between the two groups is strong also during the transfer phase, as can be claimed from the Mann-Whitney U test ($U = 4, p = 0.095$).

It appears that the two groups adopt a completely different control strategy during the first two phases of the experiment: whereas the HEH group tends to touch down with a negative pitch rate (nose-down), the EHE group shows a positive \bar{q}_{td} (nose-up). The former behavior is usually adopted in reality in order to level the skids with the ground to avoid a tail strike and have better visibility before cushioning the touchdown (Ref. 7). The EHE group aligned with the HEH group during the back-transfer phase. In order to gain more insight into this unexpected result, a detailed analysis of the control techniques adopted by the pilots of the two groups is conducted in the section Control Strategy Metrics.

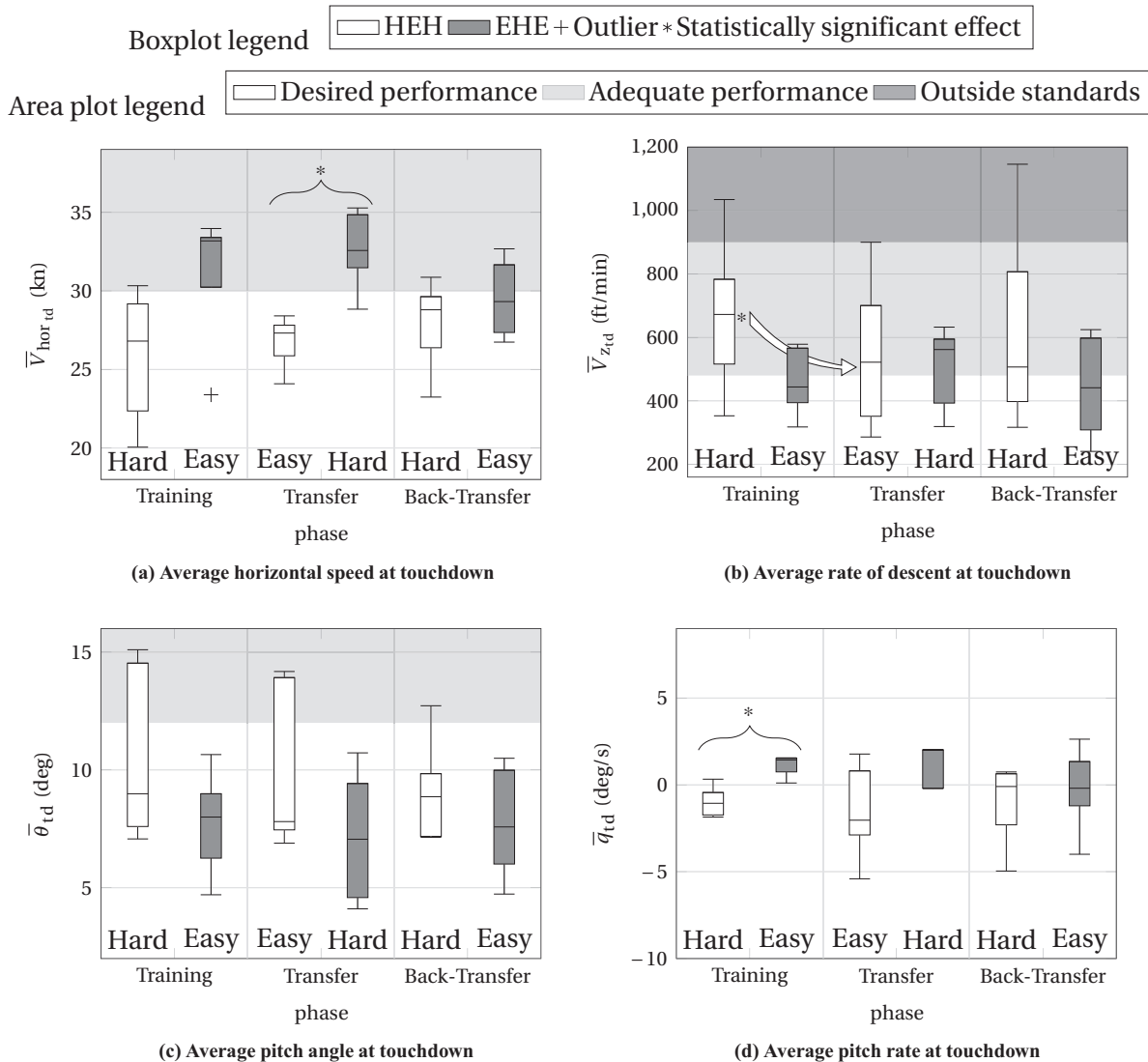


Fig. 9. Distribution of the average longitudinal performance metrics at touchdown for each group in each phase.

Figures 10(a)–10(d) show the distribution of the average roll angle $\bar{\phi}_{td}$, lateral speed \bar{v}_{td} , roll \bar{p}_{td} , and yaw \bar{r}_{td} rates at touchdown, respectively. Although the HEH group has in general a larger within-group variability, the performance in these four metrics is comparable for both groups in each experiment phase and shows little variation throughout the experiment. This is confirmed by the repeated measures ANOVA tests of Table 7 that do not show any statistically significant effects. Although not significant, the roll rate is characterized by an interaction p -value close to significance ($F(2, 16) = 3.615, p = 0.051$).

The presence of an overall significant effect in the complete data set of the average roll rate was further investigated by performing t -tests on individual sets of samples. Tables 8 and 9 illustrate the results of these tests. The only statistically significant difference that was identified concerns the transition from the transfer to the back-transfer phase of the EHE group ($t(4) = -2.797, p = 0.049$).

Touchdown precision

The relatively high average lateral speed at touchdown (Fig. 10(b)) is an indicator of the efforts made by the pilots to align with the center line

of the runway, as they were briefed to do. Figure 11 illustrates the touchdown zones for the two groups during each experiment phase, visualized with a 95% confidence ellipse. It can be noticed that both groups perform well in terms of landing precision since all the confidence ellipses almost entirely overlap with the runway.

Control strategy metrics

As for the performance metrics, the control strategy metrics (reaction time, flare initiation altitude, rotation altitude, cushion altitude, and rotor RPM at touchdown) were also averaged over the last 10 runs completed by each participant in each phase. These averaged metrics are shown in Fig. 12 as boxwhiskers plots to compare the control strategy of the two groups in the training, transfer, and back-transfer phases. From Fig. 12, it appears that the spread of results for the EHE is generally larger than the HEH group, regardless of training, transfer, or back transfer phase. The source of the larger spread for the EHE group compared to the HEH group is likely related to the fact that the EHE group seems to use more variable strategies for attaining desired performance

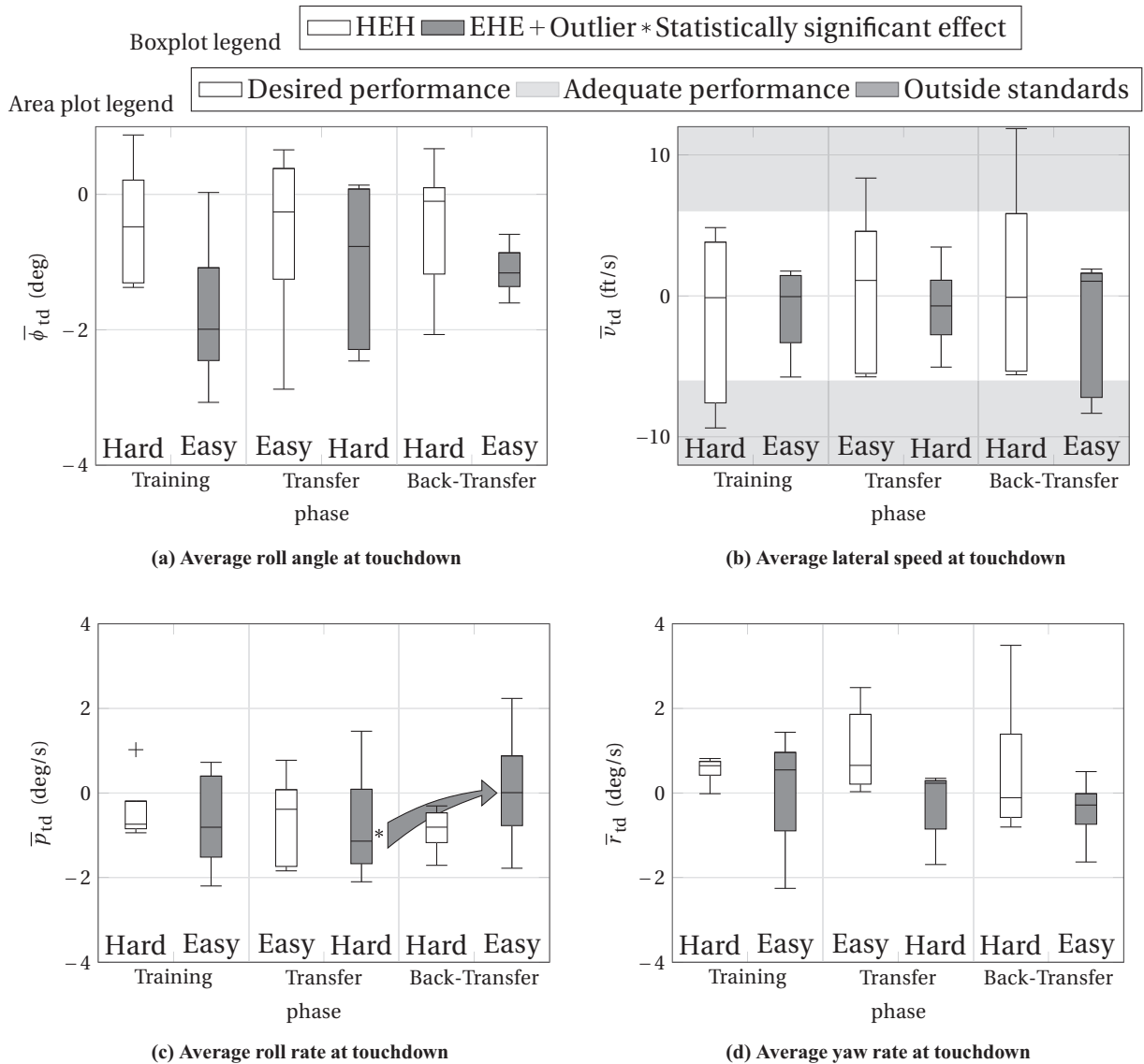


Fig. 10. Distribution of the average lateral-directional performance metrics at touchdown for each group in each phase.

(e.g., anticipate the flare, cushion the touchdown before leveling the skids).

Figure 12(a) illustrates that every participant of both groups is able to keep the average reaction time below 1 s, which is usually the value considered as the allowable pilot time delay following power failure during the certification of a civil helicopter (Ref. 72). Although the failure was random and unannounced, participants were expecting it to happen, keeping a high level of alertness. This might be the reason for such a good result in terms of reaction time.

Figure 12(b) shows the distribution of the average flare initiation altitude \bar{h}_f , which is comparable for the two groups in each experiment phase and is approximately constant at around 150 ft throughout the experiment. This is confirmed by the repeated measures ANOVA test performed on the average flare initiation altitude, which does not show any statistically significant effects (Table 7).

Some participants of the HEH group start to level the helicopter with the ground much earlier than the participants of the EHE group during the training and the transfer phases (Fig. 12(c)) to gain better visibility before cushioning the touchdown. The approach adopted by the partic-

ipants of the HEH group is successful because it prevents them from cushioning too early, which is what happens to the participants of the EHE group (Fig. 12(d)). A too early cushion will likely result in a balloon landing, that is, the helicopter regains altitude before touchdown. As a consequence, a considerable amount of rotor energy is dissipated and the loss of collective effectiveness is counteracted by starting a second flare. This explains why the EHE group exhibits lower RPM values at touchdown (Fig. 12(e)) with respect to the HEH group and positive pitch rates at touchdown (Fig. 9(d)).

For the average rotation altitude \bar{h}_{rot} (Fig. 12(c)) and the average cushion altitude \bar{h}_{cush} (Fig. 12(d)), a statistically significant interaction effect is found ($F(2, 16) = 5.855, p = 0.012$, and $F(2, 16) = 3.947, p = 0.040$, respectively), as shown in Table 7.

The presence of an overall significant effect in the complete data set of the average rotation altitude and of the average cushion altitude was further investigated by performing *t*-tests on individual sets of samples. Tables 8 and 9 illustrate the results of these tests. The only statistically significant difference that was identified for the average rotation altitude concerns the transition of the EHE group from the transfer to the

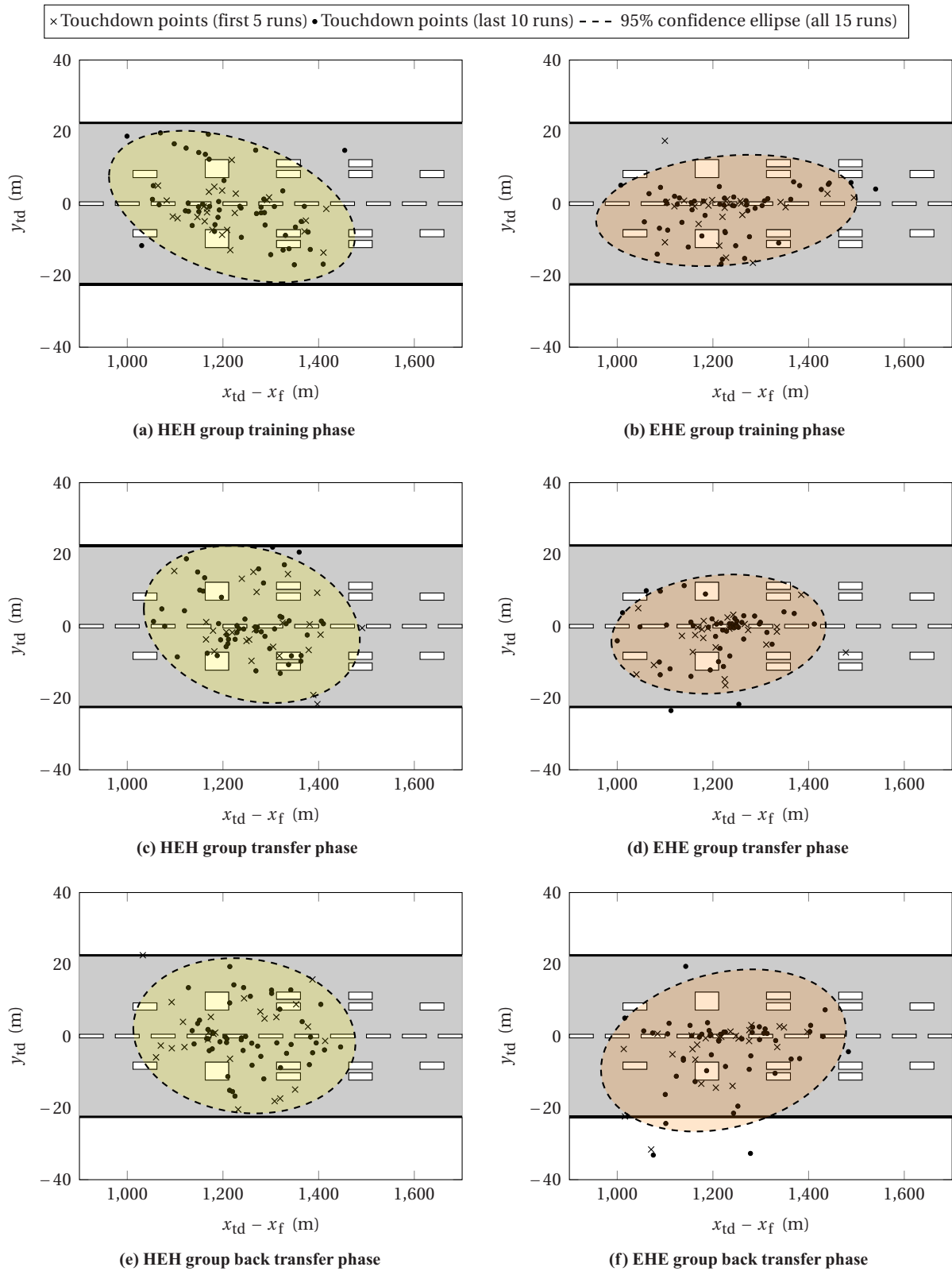


Fig. 11. Touchdown zones for the two groups during each phase visualized with a 95% confidence ellipse.

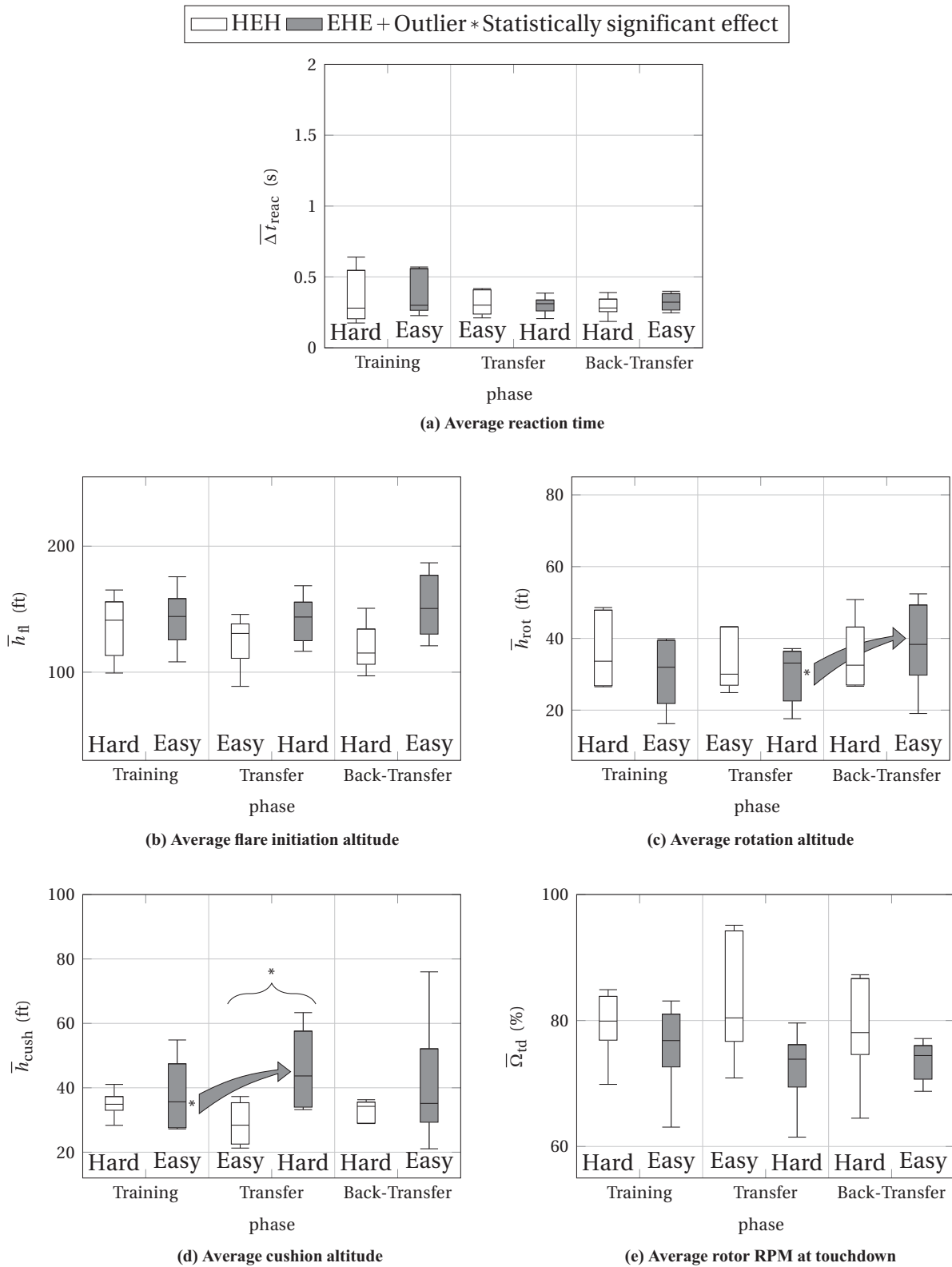


Fig. 12. Distribution of the average control strategy adopted by each group in each phase.

back-transfer phase ($t(4) = -3.414, p = 0.027$), indicating that the EHE group aligned its control strategy with that of the HEH group during the last phase of the experiment.

Concerning the average cushion altitude, Table 8 shows a statistically highly significant difference during the transition of the EHE group from the training to the transfer phase ($t(4) = -9.614, p = 0.001$) and Table 9

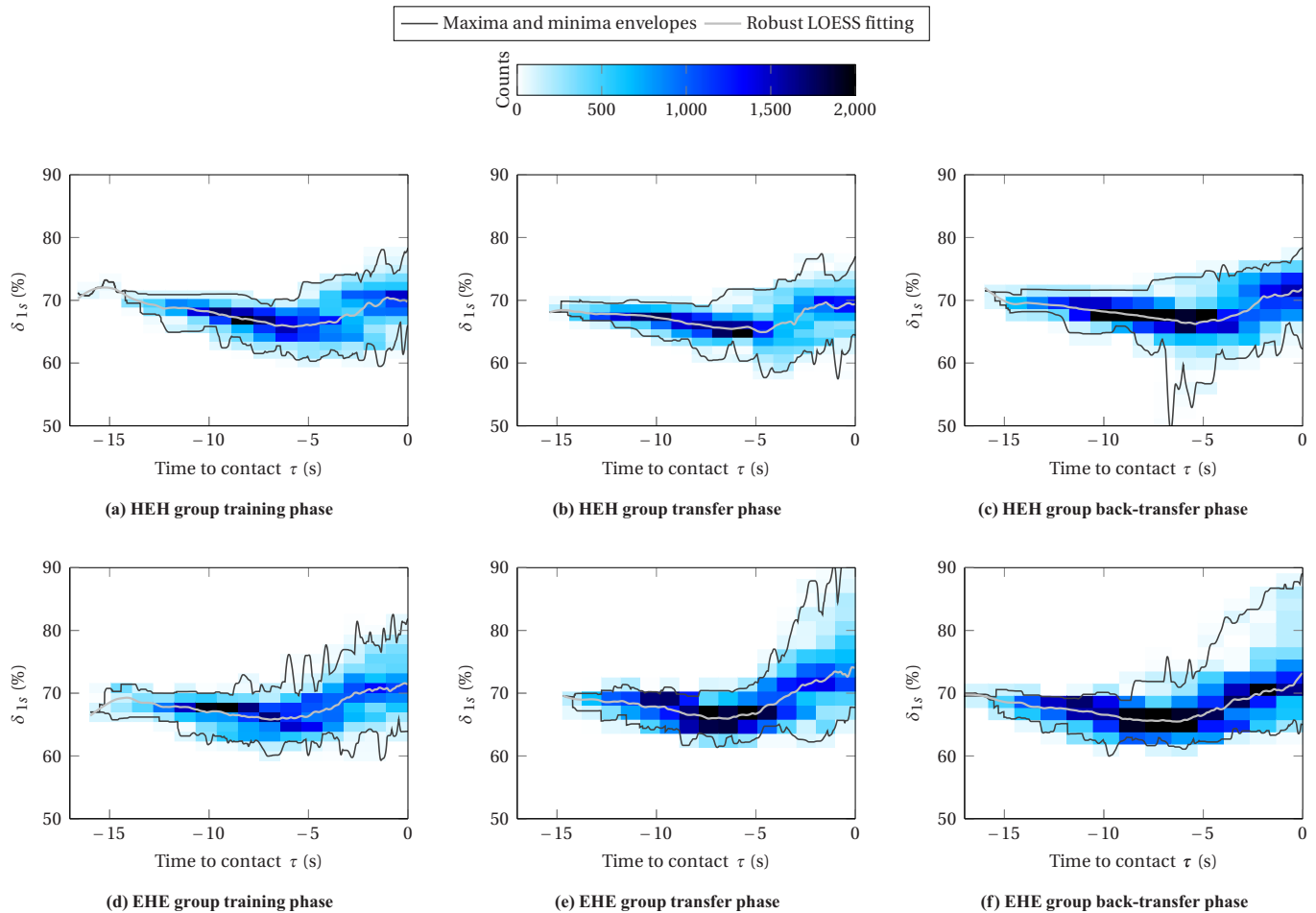


Fig. 13. Flare to touchdown longitudinal cyclic input time histories and average control strategy.

indicates a statistically significant difference between the two groups in the transfer phase ($t(8) = -2.552, p = 0.034$).

Although the EHE group exhibits lower RPM values at touchdown with respect to the HEH group, the differences between the groups in the average rotor speed at touchdown $\bar{\omega}_{td}$ are not significant and do not change significantly throughout the experiment, as summarized in Table 7.

Control strategy identification

Binned scatter plots are adopted to represent control input time histories to be able to extract meaningful information from the data of all the participants and make a fair comparison between the two groups. A binned scatter plot can be interpreted as a two-dimensional histogram or a density map and is computed by grouping a set of data points specified by their x and y coordinates into bins, and applying an aggregation function, to set the color of the tile representing the bin. The aggregation function usually counts the number of data points falling in each bin. This kind of visualization is often used to manage over-plotting, or situations where showing large data sets as scatter plots would result in points overlapping each other and hiding patterns.

The binned scatter plots of the control input time histories are shown in Figs. 13 and 14 for the longitudinal cyclic and the collective, respectively. The first row of the two figures refers to the HEH group, whereas the second one to the EHE group. Each column of the two figures refers to

a specific phase of the experiment (training, transfer, and back-transfer). Together with each binned scatter plot, also maxima and minima envelopes of the data are shown. Furthermore, a local polynomial regression fitting technique, known as robust LOESS, was used to fit the data and identify an “average” group control strategy in each phase. The two groups adopt indeed a different control strategy, especially on the collective lever. The EHE group smoothly increases the collective during the rotation phase of the flare, whereas the HEH group control strategy on the collective exhibits a step variation before touchdown. The latter behavior is more in agreement with autorotation flight-test data presented by Ref. 36.

Discussion

The quasi-transfer-of-training experiment presented in this paper expands a previous study (Ref. 46) that was designed to investigate how helicopter dynamics affect pilots’ acquisition of skills during autorotation training in a flight simulator. The promising findings from this previous experiment are based on a 4-DOF flight dynamics model with longitudinal dynamics only, and their relevance was deemed as a solid foundation to further explore this topic with a full 7-DOF flight dynamics model, which incorporates also the helicopter lateral-directional dynamics.

As in the previous experiment (Ref. 46), two sets of helicopter dynamics, characterized by a different autorotative index (hard, lower index, and easy, higher index) (Ref. 10), and two groups of participants, both

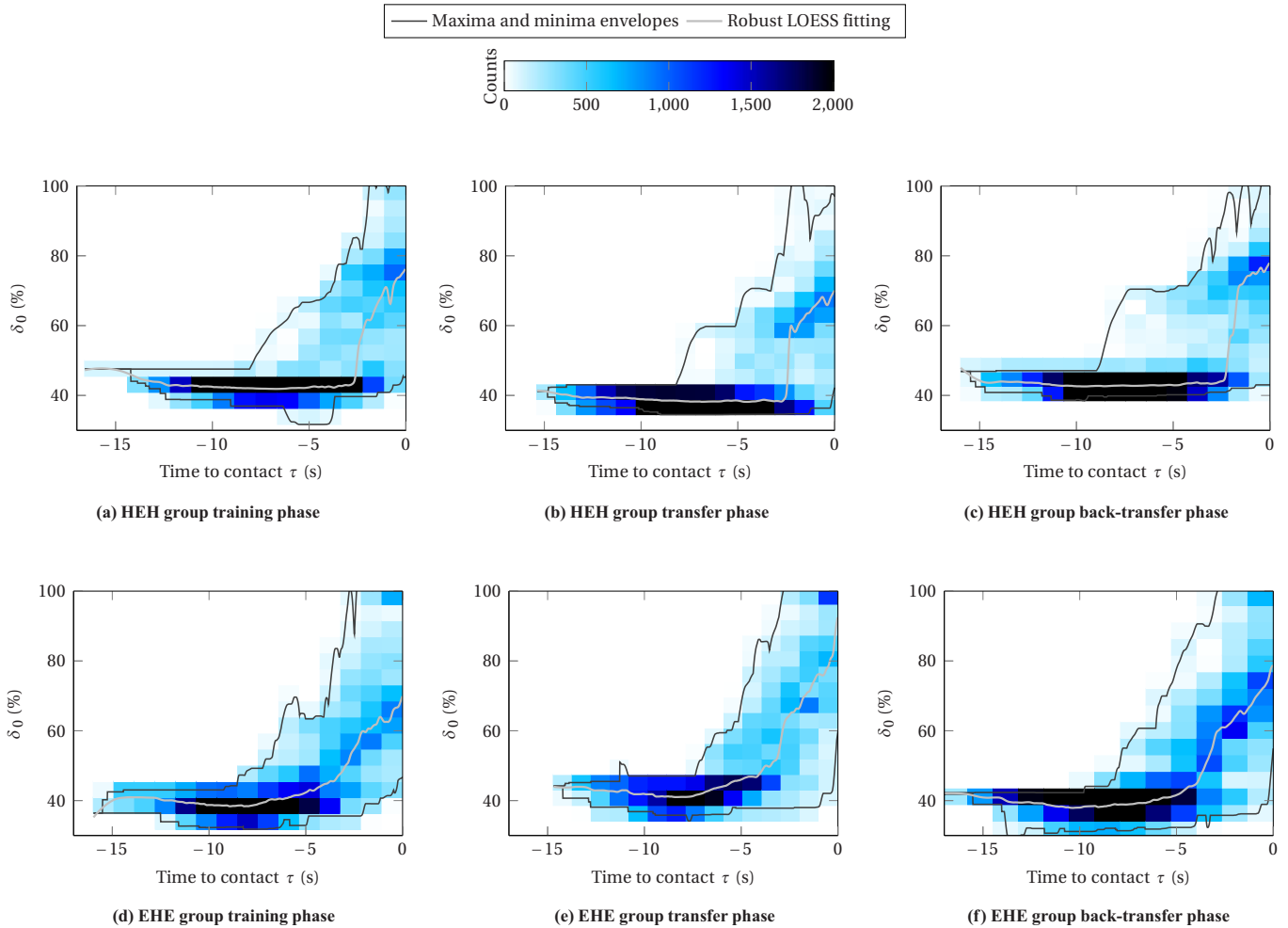


Fig. 14. Flare-to-touchdown collective input time histories and average control strategy.

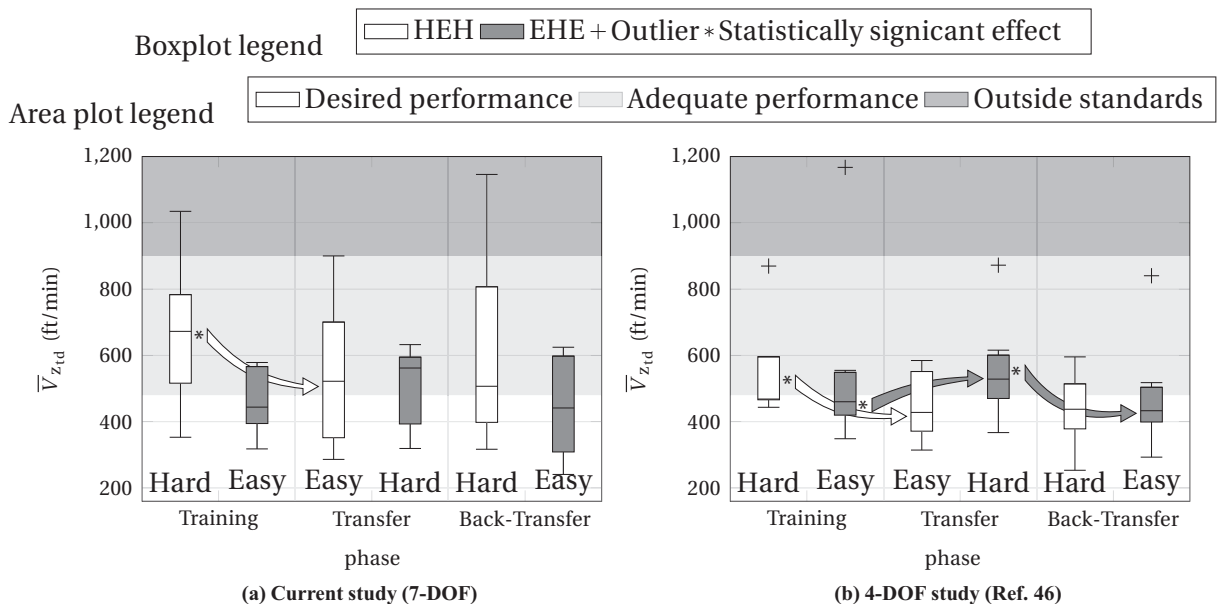


Fig. 15. Comparison of the average rate of descent at touchdown between the current study and the previous one (Ref. 46).

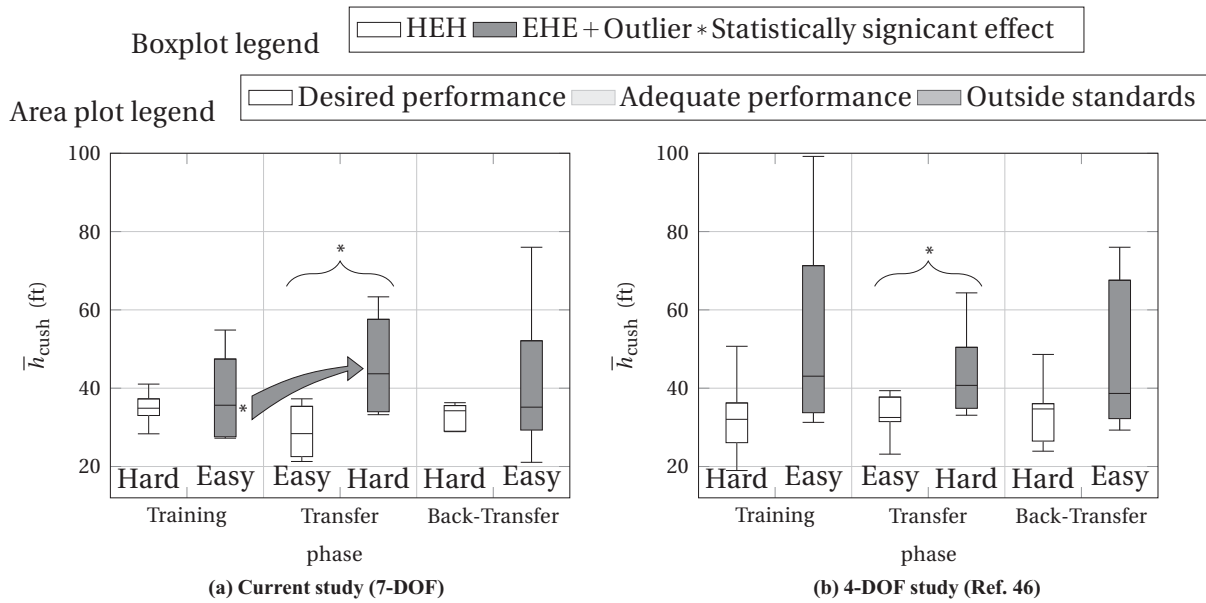


Fig. 16. Comparison of the average cushion altitude between the current study and the previous one (Ref. 46).

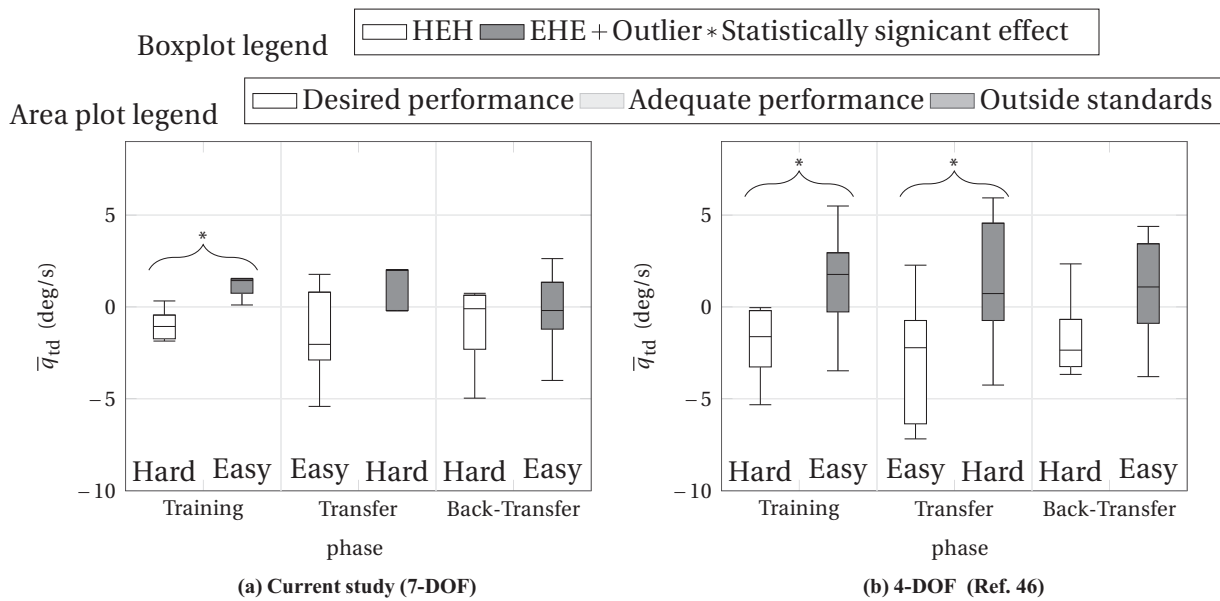


Fig. 17. Comparison of the average pitch rate at touchdown between the current study and the previous one (Ref. 46).

chosen from experienced helicopter pilots, were considered. In order to assess whether familiarity with one set of helicopter dynamics affects the learning of new helicopter dynamics, each group started the training with either the hard or the easy dynamics, was then transferred to the other, and, finally, transferred back to the initial dynamics.

The outcome of this and the previous (Ref. 46) experiments confirm previous experimental evidence which showed positive transfer of skills from agile (hard case, where high control compensation is required by the pilot) to inert (easy case, where low intervention is required by the pilot) dynamics, but not the opposite for a different training task (Ref. 48). In contrast to Ref. 48, a different definition of easy and hard is used in this and the previous experiments (Ref. 46), which is not based on the helicopter responsiveness to pilot control inputs, but on the value of the autorotative flare index. This means that the training paradigm of hard-to-easy was successfully expanded to a new training task.

Indeed, in both our experiments, both groups of participants exhibited a decrease in the rate of descent at touchdown from the hard to the easy dynamics (Fig. 15). This result corroborates our main hypothesis because a lower rate of descent is an indicator of more controlled and smoother touchdowns. The previous statement is also supported by an increase in the number of landings within adequate performance during the transfer from the hard to the easy helicopter dynamics of around 23% for the HEH group (significant effect) and 7% for the EHE group, which however was not statistically significant.

This is in agreement with current flight education, which usually starts with unaugmented helicopters at the beginning. Once proficiency is reached, later training stages involve augmented helicopters (Ref. 73).

Furthermore, results suggest that power recovery autorotations, which are the standard in civil in-flight training, may provide the pilot

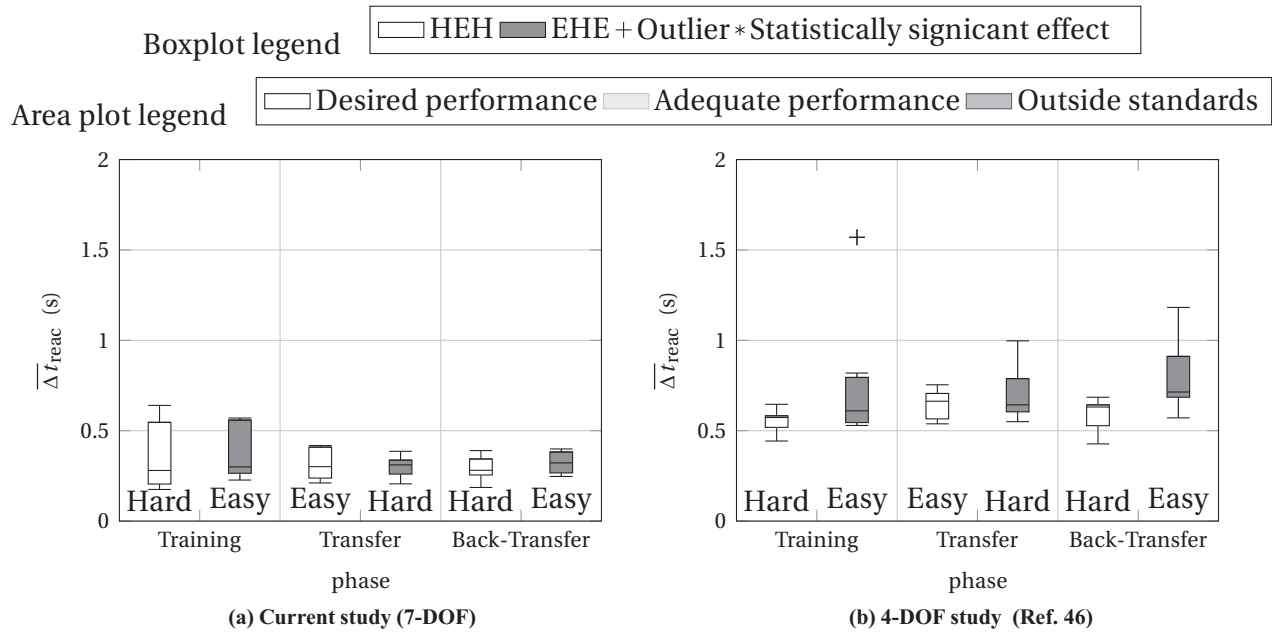


Fig. 18. Comparison of the average reaction time between the current study and the previous one (Ref. 46).

with insufficient/inadequate skills to face a real power-out situation. Indeed, even if the engine is in a ground-idle setting, some power may still be transmitted to the rotor, contributing to the generation of lift. In this circumstance, the helicopter appears lighter than it really is, thus resulting in a higher effective autorotative flare index and a possibly easier autorotation. This means that the pilot will practice simulated engine failures only with the “easy” configuration (i.e., a variation of the baseline helicopter with reduced weight to achieve a higher autorotative flare index) and, according to the outcome of this and the previous study (Ref. 46), autorotation flying skills acquired in the “easy” configuration are not positively transferred to the “hard configuration” (i.e., the baseline helicopter).

The hard helicopter dynamics foster the development of more robust and flexible flying skills because pilots are required to react faster to perceptual changes. Indeed, participants of the HEH group adopted, from the start of the experiment, a control strategy similar to the one adopted in real helicopters, as opposed to the participants of the EHE group, who tend to underestimate the altitude during the first two phases of the experiment, thus preempting the cushion (Fig. 16).

This sometimes results in a balloon landing (the helicopter gains altitude before touchdown), causing the rotor speed to drop down and the consequent loss of collective effectiveness is counteracted by starting a second flare. This is the reason why the participants of the EHE group touch down with a positive pitch rate during the training and the transfer phases (Fig. 17). However, they align their control strategy with that of the participants of the HEH group during the back-transfer phase (from the hard to the easy dynamics).

Since the final part of the autorotation is mainly a longitudinal maneuver, the use of a 3-DOF symmetrical helicopter model adopted in our previous study (Ref. 46) allows for accurate prediction in terms of pilots’ performance at touchdown (Fig. 15) and control strategy (Figs. 16 and 17). This is also confirmed by the fact that the participants of both groups succeeded in attaining desired performance at touchdown in the lateral-directional metrics almost in every run of each phase (Fig. 10).

However, the 3-DOF symmetrical helicopter model case fails to provide sufficient visual and motion cues to recognize the engine failure, due to its inability to model the initial yaw in the direction of the rotor

angular speed which follows a power failure. This is proven by the fact that the average reaction time of the participants of the previous study (≈ 0.6 s) is approximately twice as high as that of the participants of the current study (≈ 0.3 s), as shown in Fig. 18. Results in terms of control strategy and reaction time are in agreement with our secondary hypotheses.

Although participants managed to keep the reaction time below 1 s in both experiments (which is usually the value considered as pilot time delay following power failure during the certification of a civil helicopter (Ref. 72)) and although the failure was random and unannounced, the pilots were still expecting it to happen, keeping a high level of alertness. To circumvent this confounding variable and create more startle and surprise, the failure should be triggered while pilots are asked to perform secondary tasks, such as navigation procedures. Of course, this is not always feasible, because it will inevitably increase the time required by every participant to complete the experiment.

The analyzed flying task resembles more closely real operations in the current study with the 7-DOF helicopter model than in the previous one with the 4-DOF model, which was easier to control experimentally because the task is more constrained, and there is less room for pilot mistakes. Although characterized by a higher variability, the current study still provides usable results that are consistent with the previous study.

The outcomes of this and the previous experiment show that pilots trained in high-resource demanding conditions are more likely to be able to handle emergencies like engine failures in the real world, where the actual situation may easily divert from the training scenario, because they develop a more robust control technique. The current simulator training syllabus for autorotation can be updated to include several configurations with different handling characteristics, which can be obtained, for example, by considering different models of the same helicopter family, to give the trainee the opportunity to familiarize with helicopters with different sizes and dynamics. This can help inexperienced pilots to better understand that autorotation is not a “by-the-numbers” procedure and that adaptability and judgement of the pilot should always cover a prominent role in the accomplishment of the task.

Results are promising and represent a solid foundation to further extend this study. A follow-up experiment will be conducted with student

pilots to investigate if the current findings for experienced helicopter pilots also hold true for relatively inexperienced student pilots.

Conclusions

A quasi-transfer-of-training experiment with 10 experienced helicopter pilots was performed in TU Delft's SRS to compare the effects of helicopter dynamics characterized by a high autorotative flare index (hard dynamics) and low index (easy) on autorotation training in a flight simulator. Participants were divided into two groups and trained to perform a straight-in autorotation maneuver controlling a 7-DOF nonlinear helicopter model with 6-DOF rigid-body dynamics plus rotor speed. Each group tested the two sets of dynamics in a different training order: HEH group and EHE group. Results show a positive transfer of skills from the hard helicopter dynamics to the easy dynamics for both groups, with the average rate of descent at touchdown that decreases to 123 ft/min for the HEH group and 57 ft/min for the EHE group. This corroborates earlier findings that the acquisition of robust flying skills is fostered by initiating training in the most challenging setting.

In addition, participants of the EHE group adopted a suboptimal control technique during the final part of the maneuver. This is suggested by the different sign of the pitch rate at touchdown for the two groups during the first two phases of the experiment: the HEH group tends to touch down with a negative pitch rate (nose-down), whereas the EHE group shows a positive one (nose-up). The former behavior is usually adopted in reality in order to level the skids with the ground to avoid tail strike and have a better visibility before cushioning the touchdown. Dealing with the difficult dynamics helped the participants of the EHE group to align their control strategy with that of the participants of the HEH group.

These results were obtained in a simulator equipped with a 6-DOF hydraulic motion system. More research on the same topic needs to be conducted using different types of simulators, such as fixed-base simulators or simulators with motion capabilities that are beyond those of a typical training simulator, and performing true-transfer-of-training studies to further confirm the outcome of this experiment.

Although an extension of the number of pilots who performed the experiment is needed to enhance the statistical significance of the findings with 6-DOF models, results suggest that simulator training for autorotation should start with training in the most resource demanding condition. Difficult dynamics require rapid responses to perceptual changes, forcing pilots to develop more robust and adaptable flying skills. This can enhance helicopter safety as pilots will be better prepared to face unexpected events that may occur during actual flight.

Acknowledgments

We thank the 10 participants of our experiment for their efforts. This study has been carried out in the context of the European Joint Doctorate NITROS (Network for Innovative Training on Rotorcraft Safety) project, whose main goal is to enhance rotorcraft safety by addressing critical aspects of their design. This project has received funding from the European Union's Horizon 2020 research and innovation programme under the Marie Skłodowska-Curie grant agreement N° 721920.

References

- ¹U.S. Joint Helicopter Safety Analysis Team, "The Compendium Report: The U.S. JHSAT Baseline of Helicopter Accident Analysis - Volume I," Technical Report, International Helicopter Safety Team, 2011.
- ²U.S. Joint Helicopter Safety Analysis Team, "The Compendium Report: The U.S. JHSAT Baseline of Helicopter Accident Analysis -

Volume II," Technical Report, International Helicopter Safety Team, 2011.

³European Helicopter Safety Analysis Team, "EHEST Analysis of 2000–2005 European Helicopter Accidents," Technical Report, European Helicopter Safety Team, 2010.

⁴European Helicopter Safety Analysis Team, "EHEST Analysis of 2006–2010 European Helicopter Accidents," Technical Report, European Helicopter Safety Team, 2015.

⁵Rogers, S. P., and Asbury, C. N., "A Flight Training Simulator for Instructing the Helicopter Autorotation Maneuver," Technical Report NASA/FR-1372, NASA, 2000.

⁶Prouty, R. W., *Helicopter Aerodynamics Volume II*, 1st ed., Eagle Eye Solutions, 2009.

⁷Coyle, S., *The Little Book of Autorotations*, 1st ed., Eagle Eye Solutions, London, UK, 2013, p. 112.

⁸Zheng, Q., Xu, Z., Zhang, H., and Zhu, Z., "A Turbohaft Engine NMPC Scheme for Helicopter Autorotation Recovery Maneuver," *Aerospace Science and Technology*, Vol. 76, May 2018, pp. 421–432, DOI: 10.1016/j.ast.2018.01.034.

⁹Fang, X., Wang, Y., and Landry, R., "Onboard Trajectory Generation for Gyroplane Unpowered Landing Based on Optimal Lift-to-Drag Ratio Target," *Aerospace Science and Technology*, Vol. 82–83, November 2018, pp. 438–449, DOI: 10.1016/j.ast.2018.09.023.

¹⁰Fradenburgh, E. A., "Technical Notes: A Simple Autorotative Flare Index," *Journal of the American Helicopter Society*, Vol. 29, (3), July 1984, pp. 73–74, DOI: 10.4050/JAHS.29.73.

¹¹White, M. D., Cameron, N., Padfield, G. D., Lu, L., and Advani, S., "The Need for Increased Fidelity in Flight Training Devices to Address the 'Rotorcraft Loss of Control Inflight' Problem," Paper 75-2019-0323, Proceedings of the 75th Annual Forum of the Vertical Flight Society, Philadelphia, PA, May 13–16, 2019.

¹²Houston, S. S., and Brown, R. E., "Rotor-Wake Modeling for Simulation of Helicopter Flight Mechanics in Autorotation," *Journal of Aircraft*, Vol. 40, (5), September 2003, pp. 938–945, DOI: 10.2514/2.6870.

¹³Chen, R. T. N., "A Survey of Nonuniform Inflow Models for Rotorcraft Flight Dynamics and Control Applications," Technical Report NASA/TM-102219, NASA, 1990.

¹⁴Ji, H., Chen, R., Lu, L., and White, M. D., "Pilot Workload Investigation for Rotorcraft Operation in Low-Altitude Atmospheric Turbulence," *Aerospace Science and Technology*, **111**, 106567 (2021), DOI: 10.1016/j.ast.2021.106567.

¹⁵Taymourash, N., Zagaglia, D., Zanotti, A., Muscarello, V., Gibertini, G., and Quaranta, G., "Experimental Study of a Helicopter Model in Shipboard Operations," *Aerospace Science and Technology*, **115**, 106774 (2021), DOI: 10.1016/j.ast.2021.106774.

¹⁶Nikolsky, A. A., and Seckel, E., "An Analytical Study of the Steady Vertical Descent in Autorotation of Single-Rotor Helicopters," Technical Report NACA TN-1906, NACA, 1949.

¹⁷Nikolsky, A. A., and Seckel, E., "An Analysis of the Transition of a Helicopter from Hovering to Steady Autorotative Vertical Descent," Technical Report NACA TN-1907, NACA, 1949.

¹⁸Nikolsky, A. A., "The Longitudinal Stability and Control of Single Rotor Helicopters in Autorotative Forward Flight," Technical Report Princeton University Aeronautical Engineering Laboratory Report No. 215, Princeton University, 1952.

¹⁹Houston, S. S., "Longitudinal Stability of Gyroplanes," *Aeronautical Journal*, Vol. 100, (991), 1996, pp. 1–6, DOI: 10.1017/S0001924000027196.

²⁰Houston, S. S., "Validation of a Rotorcraft Mathematical Model for Autogyro Simulation," *Journal of Aircraft*, Vol. 37, (3), 2000, pp. 403–409, DOI: 10.2514/2.2640.

²¹Houston, S. S., "Analysis of Rotorcraft Flight Dynamics in Autorotation," *Journal of Guidance, Control, and Dynamics*, Vol. 25, (1), 2002, pp. 33–39, DOI: 10.2514/2.4872.

²²Houston, S. S., "Modeling and Analysis of Helicopter Flight Mechanics in Autorotation," *Journal of Aircraft*, Vol. 40, (4), July 2003, pp. 675–682, DOI: 10.2514/2.3171.

²³Chi, C., Yan, X., Chen, R., and Li, P., "Analysis of Low-Speed Height-Velocity Diagram of a Variable-Speed-Rotor Helicopter in One-Engine-Failure," *Aerospace Science and Technology*, Vol. 91, August 2019, pp. 310–320, DOI: 10.1016/j.ast.2019.05.003.

²⁴Scaramuzzino, P. F., Pavel, M. D., Pool, D. M., Stroosma, O., Quaranta, G., and Mulder, M., "Investigation of the Effects of Autorotative Flare Index Variation on Helicopter Flight Dynamics in Autorotation," Paper 89, Proceedings of the 45th European Rotorcraft Forum (ERF 2019), Warsaw, Poland, September 17–20, 2019.

²⁵Han, D., Dong, C., and Barakos, G. N., "Performance Improvement of Variable Speed Rotors by Gurney Flaps," *Aerospace Science and Technology*, Vol. 81, October 2018, pp. 118–127, DOI: 10.1016/j.ast.2018.07.044.

²⁶Seter, D., and Rosen, A., "Theoretical and Experimental Study of Axial Autorotation of Simple Rotary Decelerators," *Journal of Aircraft*, Vol. 51, (1), January 2014, pp. 236–248, DOI: 10.2514/1.C032305.

²⁷Piechocki, J., Mora, V. N., and Sanz-Andrés, Á., "Numerical Simulation of Pararotor Dynamics: Effect of Mass Displacement from Blade Plane," *Aerospace Science and Technology*, Vol. 55, August 2016, pp. 400–408, DOI: 10.1016/j.ast.2016.04.004.

²⁸Martiarena, J. F., Nadal Mora, V., and Piechocki, J., "Experimental Study of the Effect of Blade Curvature and Aspect Ratio on the Performance of a Rotary-Wing Decelerator," *Aerospace Science and Technology*, Vol. 43, June 2015, pp. 471–477, DOI: 10.1016/j.ast.2015.04.002.

²⁹Bauknecht, A., Raffel, M., and Grebing, B., "Airborne Acquisition of Blade Tip Displacements and Vortices on a Coaxial Helicopter," *Journal of Aircraft*, Vol. 55, (5), September 2018, pp. 1995–2007, DOI: 10.2514/1.C034647.

³⁰Feil, R., and Hajek, M., "Aeromechanics of a Coaxial Ultralight Rotorcraft During Turn, Climb, and Descent Flight," *Journal of Aircraft*, Vol. 58, (1), January 2021, pp. 43–52, DOI: 10.2514/1.C035684.

³¹Mulder, M., Zaal, P., Pool, D. M., Damveld, H. J., and van Paassen, M., "A Cybernetic Approach to Assess Simulator Fidelity: Looking Back and Looking Forward," Paper AIAA-2013-5225, Proceedings of the AIAA Modeling and Simulation Technologies (MST) Conference, Boston, MA, August 19–22, 2013, DOI: 10.2514/6.2013-5225.

³²Pool, D. M., Harder, G. A., and van Paassen, M. M., "Effects of Simulator Motion Feedback on Training of Skill-Based Control Behavior," *Journal of Guidance, Control, and Dynamics*, Vol. 39, (4), April 2016, pp. 889–902, DOI: 10.2514/1.G001603.

³³Binet, L., Martin, J. N., and Brackbill, C., "Autorotation maneuver analysis of main rotor and aircraft flight from engine failure to ground contact," Proceedings of the 42nd European Rotorcraft Forum 2016 (ERF2016), Association Aéronautique et Astronautique de France (3AF), Lille, France, September 5–8, 2016.

³⁴Jones, M., "An Objective Method to Determine the Fidelity of Rotorcraft Motion Platforms," Paper AIAA-2017-1082, Proceedings of the AIAA Modeling and Simulation Technologies Conference, Grapevine, TX, January 9–13, 2017, DOI: 10.2514/6.2017-1082.

³⁵Rogers, J., Eberle, B., Jump, M., and Cameron, N., "Time-to-Contact-Based Control Laws for Flare Trajectory Generation and Landing Point Tracking in Autorotation," Proceedings of the 74th Annual Forum & Technology Display of the American Helicopter Society International, Phoenix, AZ, May 14–17, 2018.

³⁶Jump, M., Alam, M., Rogers, J., and Eberle, B., "Progress in the development of a time-to-contact autorotation cueing system," Proceedings

of the 44th European Rotorcraft Forum (ERF 2018), Netherlands Association of Aeronautical Engineers (NVvL), Delft, Netherlands, September 18–20, 2018.

³⁷Decker, W., Adam, C., and Gerdes, R., "Pilot Use of Simulator Cues for Autorotation Landings," Paper 42-2-006, Proceedings of the 42nd Annual Forum of the American Helicopter Society, Washington, DC, June 2–5, 1986.

³⁸Kaiser, M., Schroeder, J., Sweet, B., and Dearing, M., "Effects of Visual Texture, Grids, and Platform Motion on Unpowered Helicopter Landings," Paper AIAA-2001-4251, Proceedings of the AIAA Modeling and Simulation Technologies Conference and Exhibit, Montreal, Canada, August 6–9, 2001, DOI: 10.2514/6.2001-4251.

³⁹McCauley, M. E., "Do Army Helicopter Training Simulators Need Motion Bases?," Technical Report 1176, U.S. Army Research Institute for the Behavioral and Social Sciences, Fort Rucker, AL, February 2006.

⁴⁰de Winter, J. C. F., Dodou, D., and Mulder, M., "Training Effectiveness of Whole Body Flight Simulator Motion: A Comprehensive Meta-Analysis," *The International Journal of Aviation Psychology*, Vol. 22, (2), April 2012, pp. 164–183, DOI: 10.1080/10508414.2012.663247.

⁴¹Zaal, P. M. T., Schroeder, J. A., and Chung, W. W., "Transfer of Training on the Vertical Motion Simulator," *Journal of Aircraft*, Vol. 52, (6), November 2015, pp. 1971–1984, DOI: 10.2514/1.C033115.

⁴²Fabbroni, D., Geluardi, S., Gerboni, C. A., Olivari, M., D'Intino, G., Pollini, L., and Bühlhoff, H. H., "Design of a Haptic Helicopter Trainer for Inexperienced Pilots," Paper 73-2017-0267, Proceedings of the 73rd Annual Forum of the American Helicopter Society, Fort Worth, TX, May 9–11, 2017.

⁴³Fabbroni, D., Geluardi, S., Gerboni, C. A., Olivari, M., Pollini, L., and Bühlhoff, H. H., "Quasi-Transfer-of-Training of Helicopter Trainer from Fixed-Base to Motion-Base Simulator," Proceedings of the 43rd European Rotorcraft Forum (ERF 2017), Milano, Italy, September 12–15, 2017.

⁴⁴Fabbroni, D., Bufalo, F., D'Intino, G., Geluardi, S., Gerboni, C. A., Olivari, M., Pollini, L., and Bühlhoff, H. H., "Transfer-of-Training: From Fixed- and Motion-Base Simulators to a Light-Weight Helicopter," Paper 74-2018-0050, Proceedings of the 74th Annual Forum of the American Helicopter Society, Phoenix, AZ, May 14–17, 2018.

⁴⁵Scaramuzzino, P. F., D'Intino, G., Geluardi, S., Pavel, M. D., Pool, D. M., Stroosma, O., Mulder, M., and Bühlhoff, H. H., "Effectiveness of a Computer-Based Helicopter Trainer for Initial Hover Training," Paper 79, Proceedings of the 44th European Rotorcraft Forum (ERF 2018), Delft, The Netherlands, September 18–21, 2018.

⁴⁶Scaramuzzino, P. F., Pavel, M. D., Pool, D. M., Stroosma, O., Mulder, M., and Quaranta, G., "Effects of Helicopter Dynamics on Autorotation Transfer of Training," *Journal of Aircraft*, Vol. 59, (1), January 2022, pp. 73–88, DOI: 10.2514/1.C036217.

⁴⁷Advisory Group for Aerospace Research and Development, "Fidelity of Simulation for Pilot Training," Technical Report AGARD-AR-159, North Atlantic Treaty Organization, Neuilly sur Seine, France, 1980.

⁴⁸Nusseck, H.-G., Teufel, H. J., Nieuwenhuizen, F. M., and Bühlhoff, H. H., "Learning System Dynamics: Transfer of Training in a Helicopter Hover Simulator," Paper AIAA-2008-7107, Proceedings of the AIAA Modeling and Simulation Technologies Conference and Exhibit, Honolulu, HI, August 18–21, 2008, DOI: 10.2514/6.2008-7107.

⁴⁹Timson, E., Perfect, P., White, M., Padfield, G., Erdos, R., and Gubbels, W., "Pilot Sensitivity to Flight Model Dynamics in Rotorcraft Simulation," Paper 172, Proceedings of the 37th European Rotorcraft Forum (ERF 2011), Vergiate and Gallarate, Italy, September 13–15, 2011.

⁵⁰Pavel, M. D., White, M., Padfield, G. D., Roth, G., Hamers, M., and Taghizad, A., "Validation of Mathematical Models for Helicopter Flight Simulators Past, Present and Future Challenges," *The Aeronautical Journal*, Vol. 117, (1190), April 2013, pp. 343–388, DOI: 10.1017/S0001924000008058.

⁵¹Hosman, R., "Are Criteria for Motion Cueing and Time Delays Possible?" Paper AIAA-99-4028, Proceedings of the Modeling and Simulation Technologies Conference and Exhibit, Portland, OR, August 9–11, 1999, DOI: 10.2514/6.1999-4028.

⁵²Hettinger, L. J. and Haas, M., *Virtual and Adaptive Environments—Applications, Implications, and Human Performance Issues*, Lawrence Erlbaum Associates, Inc., Mahwah, New Jersey, 2003, ISBN 0-8058-3107-X.

⁵³US Army AMCOM, "Aeronautical Design Standard-33E-PRF, Performance Specification, Handling Qualities Requirements for Military Rotorcraft," Technical Report, U.S. Army AMCOM, Redstone Arsenal, AL, 2000.

⁵⁴Porcaccia, F., Riccardi, F., Mancini, A., Pecoraro, M., Ragazzi, A., and Viganò, L., "Assessment of numerical approaches for modelling tilt-rotor ground effect stability in hover and near hover conditions," Proceedings of the 79th Annual Forum of the Vertical Flight Society, West Palm Beach, FL, May 16–18, 2023.

⁵⁵European Aviation Safety Agency, "Means of Compliance with the Special Condition VTOL," Technical Report First publication MOC SC-VTOL, Issue 1, EASA, 2020.

⁵⁶Berger, T., Blanken, C. L., Tischler, M. B., and Horn, J. F., "Flight Control Design and Simulation Handling Qualities Assessment of High-Speed Rotorcraft," Proceedings of the 75th Annual Forum and Technology Display of the Vertical Flight Society, Philadelphia, PA, May 13–16, 2019.

⁵⁷Saetti, U., Horn, J. F., Berger, T., and Tischler, M. B., "Rotorcraft Flight Control Design with Alleviation of Unsteady Rotor Loads," Proceedings of the 75th Annual Forum and Technology Display of the Vertical Flight Society, Philadelphia, PA, May 13–16, 2019.

⁵⁸Sunberg, Z. N., Miller, N. R., and Rogers, J. D., "A Real-Time Expert Control System for Helicopter Autorotation," *Journal of the American Helicopter Society*, Vol. 60, (2), April 2015, pp. 1–15, DOI: 10.4050/JAHS.60.022008.

⁵⁹Sunberg, Z. N., Miller, N. R., and Rogers, J. D., "A Real Time Expert Control System for Helicopter Autorotation," Paper 70-2014-0201, Proceedings of the 70th Annual Forum of the American Helicopter Society, Montréal, Québec, May 20–22, 2014.

⁶⁰Department of the Air Force and Navy Bureau of Aeronautics, "Military Specification - Structural Design Requirements, Helicopters,"

Technical Report MIL-S-8698, Department of the Air Force and Navy Bureau of Aeronautics, 1954.

⁶¹Department of the Army, "Engineering Design Handbook, Helicopter Engineering, Part I - Preliminary Design," Technical Report AMCP 706-201, Department of the Army, 1974.

⁶²Crist, D., and Symes, L., "Helicopter Landing Gear Design and Test Criteria Investigation," Technical Report USAVRADCOM-TR-81-D-15, Bell Helicopter Textron, 1981.

⁶³Talbot, P. D., Tinling, B. E., Decker, W. A., and Chen, R. T. N., "A Mathematical Model of a Single Main Rotor Helicopter for Piloted Simulation," Technical Report NASA/TM-84281, NASA, 1982.

⁶⁴Murakami, Y., and Houston, S. S., "Dynamic Inflow Modelling for Autorotating Rotors," *Aeronautical Journal*, Vol. 112, 2008, pp. 47–53, DOI: 10.1017/S0001924000001986.

⁶⁵Padfield, G. D., *Helicopter Flight Dynamics: The Theory and Application of Flying Qualities and Simulation Modelling*, 2nd ed., Blackwell Publishing Ltd, Oxford, UK, 2007, DOI: 10.1002/9780470691847.

⁶⁶Stroosma, O., van Paassen, R., and Mulder, M., "Using the SIMONA Research Simulator for Human-Machine Interaction Research," Paper AIAA-2003-5525, Proceedings of the AIAA Modeling and Simulation Technologies Conference and Exhibit, Austin, TX, August 11–14, 2003, DOI: 10.2514/6.2003-5525.

⁶⁷Miletovic, I., Pavel, M. D., Stroosma, O., Pool, D. M., Van Paassen, M. M., Wentink, M., and Mulder, M., "Eigenmode Distortion as a Novel Criterion for Motion Cueing Fidelity in Rotorcraft Flight Simulation," Paper 45, Proceedings of the 44th European Rotorcraft Forum 2018 (ERF 2018), Delft, The Netherlands, September 18–21, 2018.

⁶⁸Reid, L. D., and Nahon, M. A., "Flight Simulation Motion-Base Drive Algorithms. Part 1: Developing and Testing the Equations," Technical Report UTIAS 296, University of Toronto, Institute for Aerospace Studies, December 1985.

⁶⁹Reid, L. D., and Nahon, M. A., "Flight Simulation Motion-Base Drive Algorithms. Part 2: Selecting the System Parameters," Technical Report UTIAS 307, University of Toronto, Institute for Aerospace Studies, May 1986.

⁷⁰Grant, P. R., and Reid, L. D., "Motion Washout Filter Tuning: Rules and Requirements," *Journal of Aircraft*, Vol. 34, (2), March 1997, pp. 145–151, DOI: 10.2514/2.2158.

⁷¹Field, A., *Discovering Statistics Using IBM SPSS Statistics*, Sage, Thousand Oaks, CA, 2013.

⁷²Prouty, R. W., *Helicopter Performance, Stability, and Control*, Krieger Publishing Company, Malabar, FL, 2002.

⁷³Coyle, S., *Cyclic & Collective - More Art and Science of Flying Helicopters*, Eagle Eye Solutions, London, UK, 2008.